Summary of Professional Accomplishments:

Electron - electron interactions in crystals containing transition metal ions

Anna Ciechan

ORCID Numer: 0000-0003-4623-960X
ResearcherID: G-1458-2012

Institute of Physics
of Polish Academy of Sciences

Contents

1 Name

Anna Ciechan

2 Diplomas and degrees conferred

25.10.2010 Degrees conferred: **doctor of physical sciences**
Maria Curie-Sklodowska University in Lublin
PhD dissertation: *„Thermodynamic properties of small, inhomogeneous and multiband superconductors"*
Supervisor: prof. dr hab. K. I. Wysokiński
(the work was defended with distinction)

10.09.2004 Degrees conferred: **master**, speciality: **theoretical physics**
Maria Curie-Sklodowska University in Lublin
Master Thesis: *„Relativistic effects in superconductors"*
Supervisor: prof. dr hab. K. I. Wysokiński

3 Information on employment in research institutes

15.11.2010 - 31.08.2023 / 01.12.2023 - . . . Institute of Physics of Polish Academy of Sciences
Division of Physics of Magnetism
Group of phase transitions
Position: **assistant professor/assistant**

4 Description of the achievements, set out in art. 219 para 1 point 2 of the Act

4.1 Title of scientific achievement

Electron-electron interaction in crystals containing transition metal ions

4.2 Scientific publications that are the basis of scientific achievement

[H1] A. Ciechan, M. J. Winiarski and M. Samsel-Czekała
„Magnetic phase transitions and superconductivity in strained FeTe"
Journal of Physics: Condensed Matter **26**, 025702 (2014)

[H2] A. Ciechan, M. J. Winiarski and M. Samsel-Czekała
„Magnetism and superconductivity of S-substituted FeTe"
Journal of Alloys and Compounds **630**, 100 (2015)

[H3] A. Ciechan, P. Dłużewski, S. Kret, K. Gas, L. Scheffler, C. Gould, J. Kleinlein, M. Sawicki, L. W. Molenkamp, and P. Bogusławski
„Coexistence of antiferromagnetic cubic and ferromagnetic tetragonal polymorphs in epitaxial CuMnSb films"
Physical Review B **110**, 014436 (2024)

[H4] A. Ciechan, P. Bogusławki
„Transition metal ions in ZnO: Effects of intrashell coulomb repulsion on electronic properties"
Optical Materials **79**, 264-268 (2018)

[H5] A. Ciechan, P. Bogusławski
„Calculated optical properties of Co in ZnO: internal and ionization transitions"
Journal of Physics: Condensed Matter **31**, 255501 (2019)

[H6] A. Ciechan, H. Przybylińska, P. Bogusławski, A. Suchocki, A. Grochot, A. Mycielski, P. Skupiński, and K. Grasza
„Metastability of Mn^{3+} in ZnO driven by strong d(Mn) intrashell Coulomb repulsion: experiment and theory"
Physical Review B **94**, 165143 (2016)

[H7] J. Papierska, A. Ciechan, P. Bogusławski, M. Boshta, M. M. Gomaa, E. Chikoidze, Y. Dumont, A. Drabińska, H. Przybylińska, A. Gardias, J. Szczytko, A. Twardowski, M. Tokarczyk, G. Kowalski, B. Witkowski, K. Sawicki, W. Pacuski, M. Nawrocki, and J. Suffczyński
„Fe dopant in ZnO: 2+ versus 3+ valency and ion-carrier $s, p-d$ exchange interaction"
Physical Review B **94**, 224414 (2016)

[H8] A. Ciechan, P. Bogusławski
„Theory of the $sp-d$ coupling of transition metal impurities with free carriers in ZnO"
Scientific Reports **11**, 3848 (2021)

4.3 Description of the scientific achievement

4.3.1 Motivation

The subject of the scientific achievement is description of electron - electron interactions in crystals containing transition metal ions (TM). Systems with different electronic structures are analyzed: metals, semimetals and semiconductors. TM ions are both components of the crystals and also occur in the form of point defects or intentional dopants introduced into materials in order to change their physical and chemical properties.

Defects and dopants change the carrier concentration of the materials, thus influencing their transport properties. The states introduced by TM ions, visible in the band structure, lead to changes in the optical properties of materials. Ions with a partially filled d shell are usually characterized by a non-zero magnetic moments and then act as magnetic dopants. If magnetic moments localized on such ions are ordered by the exchange interactions and/or by external magnetic field, they lead to the appearance of collective magnetic order in the system, e.g. ferro- or antiferromagnetism.

For this reason, transition metal ions are the subject of extensive theoretical and experimental studies aimed at examining changes in the electrical, optical and magnetic properties of materials, i.e. properties important for applications. In particular, physics of TM dopants is the subject of research at the Institute of Physics of the Polish Academy of Sciences (IP PAS), as well as at the Faculty of Physics of the University of Warsaw, at the Institute of Low Temperatures and Structural Research of the Polish Academy of Sciences in Wroclaw and cooperating foreign groups from the National Research Center in Giza (Egypt), the University of Versailles St-Quentin in Yvelines-CNRS (France) and the University of Würzburg (Germany).

The description of transition metal ions is a challenge and a motivation for theoretical research. In density functional theory (DFT) calculations, standard approximations used for exchange-correlation interactions fail in many situations and need to be improved to properly describe the electronic structure of the considered crystals and the resulting properties. At the same time, such calculations allow for a deeper analysis of the interactions occurring in the crystal, in particular the intrashell interactions of d(TM) electrons and the interactions of the d(TM) electrons with the remaining valence electrons in the system.

In this scientific achievement, transition metal ions in three classes of materials were investigated. They include metallic compounds as iron chalcogenide FeTe and half-Heusler alloy CuMnSb as well as wide-gap semiconductor ZnO. In each case, the results obtained within DFT calculations were confronted with experiment in order to select the appropriate method necessary for the correct description of a given class of materials.

(1) *Magnetic and superconducting FeTe phases.*

Iron chalcogenides, Fe(Se,Te), are the simplest in composition and therefore the easiest to theoretical study iron-based superconductors [1]. Available experimental and theoretical results clearly indicate that antiferromagnetic fluctuations associated with the electronic band structure have a significant effect on the superconducting state of iron pnictides and iron chalcogenides. Partial substitution of Te in

superconducting FeSe increases its critical temperature [2], however, pure FeTe is antiferromagnetic [3]. Moreover, magnetic order of FeTe transforms from antiferromagnetic into the ferromagnetic under external pressure [4]. Superconductivity in FeTe is induced by partial substitution of selenium or sulfur at the Te positions [2, 5] and by strains in epitaxial FeTe layers on $SrTiO_3$ and MgO substrates [6]. The motivation for undertaking theoretical studies presented in [H1, H2] was to investigate the FeTe phase transitions induced by substitutions and hydrostatic and axial pressure.

(2) *Antiferromagnetic half-Heusler CuMnSb.*

CuMnX compounds (X = P, As and Sb) exhibit antiferromagnetic order at low temperatures and play an important role in the currently developing field of spintronics based on antiferromagnetism [7]. In epitaxial CuMnSb films, a ferromagnetic contribution is also visible, which disappears at temperatures higher than the antiferromagnetic order. Simultaneously, coexistence of two structural polymorphs is observed, i.e. the dominant cubic structure and additional tetragonal inclusions. The motivation of the work [H3] was to explain the observed effects, in particular to investigate the relationship between the coexistence of two magnetic phases and two crystallographic phases in CuMnSb films. Analysis of the results obtained from DFT calculations based on the model Hamiltonian (with short-range magnetic coupling described by the Heisenberg model and long-range coupling of the RKKY type) allowed further insight into the mechanisms of exchange interactions in this material.

(3) *TM ions in wide-gap semiconductors like ZnO.*

Wide-bandgap semiconductors are intensively studied for applications in optoelectronics and photovoltaics, or in hydrogen production in water splitting processes [8]. Magnetically doped II-VI semiconductors are also of interest due to their potential use in spintronics or solotronics [9, 10]. Such systems provide a unique opportunity to change the charge state of TM ions by changing the energy of the Fermi level. The charge state affects the occupancy of the d(TM) shell and, consequently, changes the energies of the d(TM) levels, the magnetic state of the ion, intrashell interactions and $s, p-d$ interactions with band carriers. The undertaken research includes the ZnO semiconductor with dopants of transition metals from Ti to Cu [H4-H8]. The motivation for this study was to explain the experimental results related to these ions. The aim was to determine the possible charge and spin states of TM ions, dopant levels, ionization energies and other properties necessary for a complete characterization of these materials. The analysis of different ions and different charge states provided insight into the fundamental mechanisms of interactions for d(TM) electrons.

The result of the scientific achievement is a theoretical description of the electron-electron interaction of selected materials containing transition metal ions. The properties of TM ions in various environments and their influence on the properties of host materials were shown, with particular emphasis on optical and magnetic characteristics.

Section 4.3.2 presents calculation methods including the $+U$ correction used in some materials. Then, in section 4.3.3 the results obtained in each of the papers [H1-H8] are discussed. Finally, a summary of the achievements is provided in section 4.3.4.

4.3.2 Calculation method: DFT and $+U$ correction

Density functional theory is a powerful tool for theoretical description of the properties of condensed matter. Hohenberg and Kohn showed [11] that the total energy of a multi-electron system is uniquely determined by the electron density, i.e. it is a functional of the density $\rho(\mathbf{r})$. In the Kohn-Sham [12] construction, the energy functional can be written in the form:

$$E[\rho] = T[\rho] + V_{ext}[\rho] + \frac{1}{2}\int \frac{\rho(\mathbf{r})\rho(\mathbf{r'})}{|\mathbf{r}-\mathbf{r'}|} d\mathbf{r}d\mathbf{r'} + E_{xc}[\rho], \tag{1}$$

in which the first term is the kinetic energy of the non-interacting particle system, the second term is the external potential coming from the atomic nuclei, and the third term describes the standard Coulomb interaction. The last term is the so-called exchange-correlation energy, related to the asymmetry of the wave function and other complexities of the many-body system. It should be emphasized here that DFT is an exact theory, but it does not provide a recipe for constructing the exchange-correlation energy $E_{xc}[\rho]$.

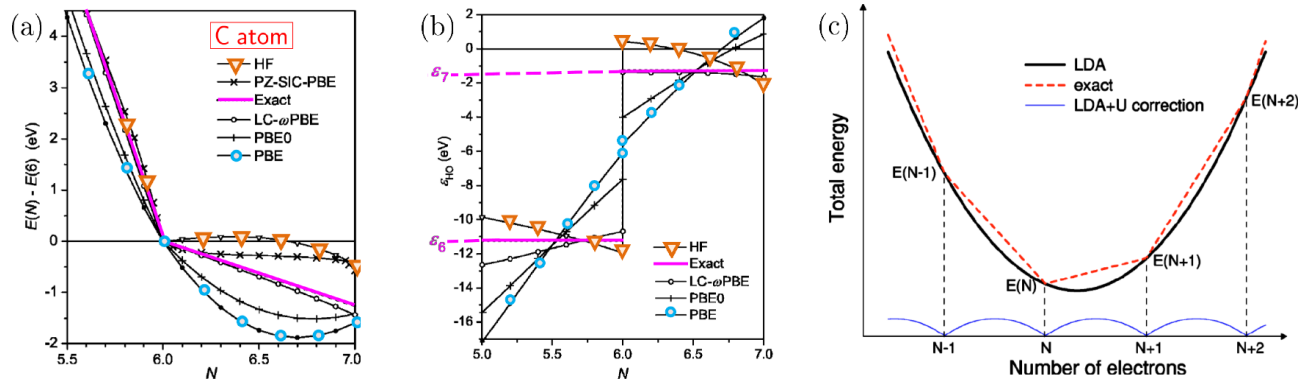

Figure 1: (a) Total energy and (b) the highest occupied state of the carbon atom as a function of the number of electrons in the system. Results obtained by the Hartree-Fock, HF, and DFT methods using several functionals, including PBE, are shown. The "exact" result is obtained from experimental ionization energy and electron affinity. Both figures are from [15]. (c) Typical dependence of the total energy on the number of electrons obtained within the LDA approximation and expected when using the exact energy functional. The $+U$ correction shown on the lower curve is the difference between the LDA and the exact result. The figure is from [18].

The Kohn-Sham mapping of interacting to non-interacting system of particles leads to the single-particle equations

$$(-\frac{\hbar^2}{2m}\nabla^2 + \upsilon_S)\varphi_i(\mathbf{r}) = \varepsilon_i\varphi_i(\mathbf{r}) \tag{2}$$

for electrons moving in an effective potential

$$\upsilon_S(\mathbf{r}) = \upsilon_{ext}(\mathbf{r}) + \frac{e^2}{2}\int \frac{\rho(\mathbf{r'})}{|\mathbf{r}-\mathbf{r'}|}d\mathbf{r'} + \upsilon_{xc}(\mathbf{r}). \tag{3}$$

Kohn-Sham states are in principle auxiliary states that allow finding the minimum of total energy, but they are identified with physical states describing single electrons in the materials. Indeed, the band structure obtained from Kohn-Sham states reproduces the experimental band structure if exchange-correlation potential is an appropriately constructed.

The DFT theory has been generalized to systems with a fractional number of particles N. According to Janak theorem [13], the single-particle states ε_i from equations (2) can be calculated as the derivative of the total energy after occupation of this state n_i

$$\varepsilon_i = \partial E/\partial n_i. \tag{4}$$

It was shown [14] that the dependence of the total energy on the number of electrons between successive total occupancies, N and $(N+1)$, should be linear

$$E(N+n) = (1-n)E_N + nE_{N+1}, \qquad n \in \langle 0,1\rangle. \tag{5}$$

With respect to an isolated atom, such a dependence gives the correct energy distance between the highest occupied state (HOMO), calculated as $\varepsilon_{HO} = \partial E/\partial N$ in the range $\langle N-1, N\rangle$, and the lowest unoccupied state (LUMO), $\varepsilon_{LU} = \partial E/\partial N$, calculated in the range $\langle N, N+1\rangle$. Importantly, HOMO-LUMO energies are closely related to the ionization energy and electron affinity energy. An example of the exact dependence of the total energy and single-particle states on the number of electrons in a carbon atom is shown in Figure 1 (a) and (b) [15].

The $E(N+n)$ dependence obtained in DFT calculations is nonlinear within the standard approximations for exchange-correlation potentials, i.e. the local density approximation (LDA) and the generalized gradient approximation (GGA) [16, 17]. Deviations related to the approximations used are visible in the results obtained for the isolated carbon atom [15]. Figures 1 (a) and (b) show the results of GGA in the method proposed by Perdew, Burke and Ernzerhof (PBE). The difference in total energy of the ionized and the charge neutral state of carbon $E(7)-E(6)$ is close to experiment, but the function $E(N)$ shows an

energy minimum for a fractional number of particles. Moreover, the dependence $E(N)$ is upward-curved, which causes changes in the position of single-particle states with increasing occupation $\varepsilon_i(N)$ and leads to the disappearance of the HOMO-LUMO gap ($\varepsilon_7 - \varepsilon_6$, at the point N =6). The figures also show the results obtained using the Hartree-Fock variational method, for which the total energy is always higher than expected and the downward-curved dependence $E(N)$ leads to too large energy distance between single-particle states $\varepsilon(6)$ and $\varepsilon(7)$.

Moving on to condensed matter physics, DFT methods with standard approximations also often fail to reproduce the electronic band structure and other properties of materials. In the case of semiconductors and insulators, the upward-curved $E(N)$ dependence leads to too narrow an energy gap between the valence band maximum and the conduction band minimum. In the works in which the LDA and GGA methods turned out to be insufficient [H3-H8], the GGA+U method was used, i.e. the GGA potential was improved by introducing an additional $+U$ term. It gives an additional V_U contribution to the Kohn-Sham potential [18]:

$$V_U|\psi^\sigma_{k\nu}\rangle = U\sum_{m,\sigma}(1/2 - \lambda^\sigma_m)|\phi_m\rangle\langle\phi_m|\psi^\sigma_{k\nu}\rangle, \tag{6}$$

where ϕ_m are orbitals localized on a given atom and occupied by λ^σ_m electrons, and $\psi^\sigma_{k\nu}$ are Kohn-Sham states determined for the wave vector k, band ν and spin σ. The potential V_U changes all single-particle states (k, ν, σ) for which the corrected orbitals contribute. At the same time, the correction to the total energy of the system associated with the $+U$ term is:

$$E_U = \frac{U}{2}\sum_{m,\sigma}\left[\lambda^\sigma_m(1 - \lambda^\sigma_m)\right]. \tag{7}$$

The impact of $+U$ correction on the $E(N)$ dependence is schematically presented in Figure 1 (c) [18]. It does not change the total energy of the system with integer number of electrons, while for fractional number of electrons it gives contributions that change the $E(N)$ dependence from parabolic, obtained from LDA or GGA, to more linear. The energy correction E_U indicates that the $+U$ contribution favors fully occupied and fully empty orbitals rather than partially occupied ones. It affects the single-particle states, shifting the filled states towards lower energies and the empty states towards higher energies, see equation (6). The $+U$ correction is usually fitted to experimental results or calculated, for example, from linear response theory [18]. Both approaches were used in the works discussed here, in which the GGA+U method was applied.

It is worth mentioning that the use of the $+U$ correction is one of the simplest methods that allow for a better description of the band structure of semiconductors. It is of great importance in the case of disordered systems (e.g. doped systems), where the efficiency of calculations is important. The selection of a specific method for the material and studied properties was dictated by the agreement of the obtained results with experiment.

In the case of iron telluride FeTe [H1, H2] the GGA approximation was used. Both LDA and GGA approximations were standarly used by many authors [19], including me and my collaborators from Institute of Low Temperature and Structural Research of Polish Academy of Sciences in calculations of the electronic band structure of iron chalcogenides [20, 21, 22]. The GGA method (unlike LDA) correctly reproduced the observed change of the magnetic order of FeTe from antiferromagnetic to ferromagnetic under the influence of hydrostatic pressure [H1].

Half-Heusler CuMnSb alloy considered in [H3] is a metal in which mainly magnetic properties were studied. The antiferromagnetic spin order in the ground state is obtained using both GGA and GGA+U methods. However, the relatively narrow bands formed by the d(Mn) orbitals and the available literature [23] suggested adding an appropriate correction to d(Mn) electrons. Finally, for both CuMnSb and Mn defects in this compound, the correction U(Mn) = 1 eV was applied. Such correction reproduces the cohesive energy of bulk manganese and gives the proper heat of formation of MnSb, considered in the work of [H3] to determine the chemical potential for Cu and Mn in CuMnSb.

The last material studied in the scientific achievement is ZnO [H4-H8]. The LDA method, as well as the GGA one, turned out to be insufficient for describing the electronic band structure of this semiconductor. These approximations give a too narrow energy gap (about 1 eV instead of 3.3 eV), as well as other deviations from the experimentally observed band structure, see Figure 2 (a). Consequently, also

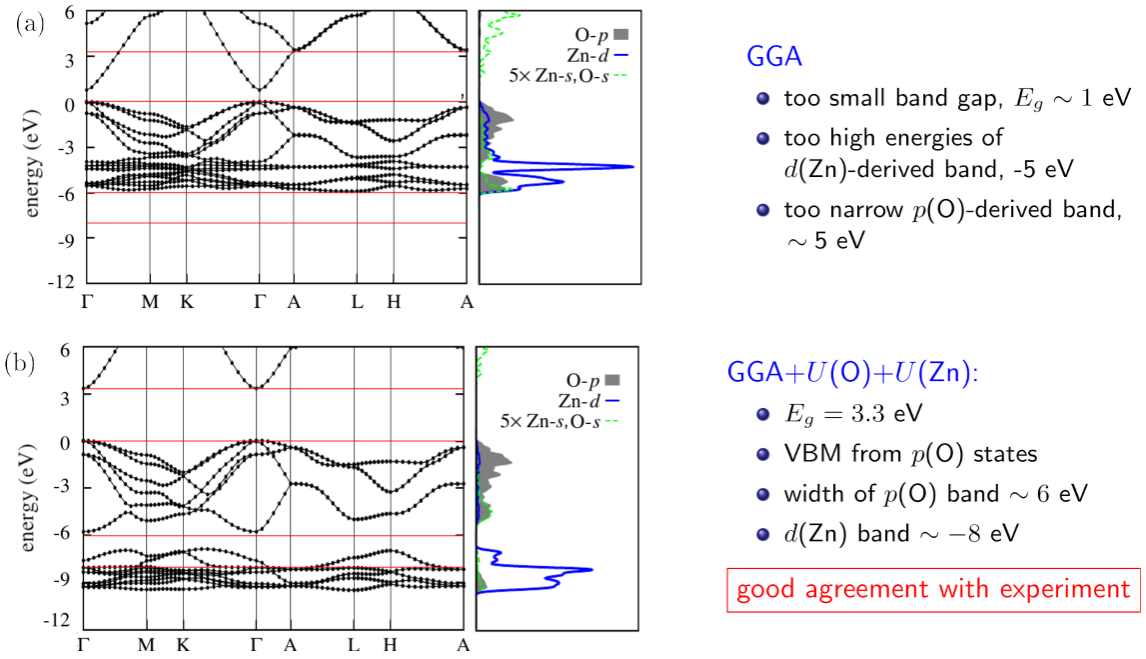

Figure 2: Band structure of ZnO obtained by (a) GGA and (b) GGA+U methods. Characteristics obtained by both methods are listed on the right.

the description of TM ions in ZnO is incorrect [24]. Due to the too narrow gap, the LDA and GGA methods often give impurity levels degenerate with the conduction band, instead of states in the gap. Then, we observe the autoionization of the impurity electron into the conduction band. As a consequence, we obtain incorrect transport properties of the system (metallic sample) and incorrect charge and spin state of the ion, and therefore wrong optical transitions and magnetic interactions.

In order to correctly describe the electronic properties of ZnO and TM impurities in ZnO, the $+U$ method was used. The works [14, 15, 18] clearly indicate that (contrary to common practice) the $+U$ corrections should be applied not only to d(TM) orbitals, but to all atomic orbitals relevant to a given problem. The band structure of ZnO is a good illustration of the above principle. Figure 2 (a), shows that the states around the gap are mainly composed of p(O) orbitals. The band formed by d(Zn) orbitals lies just below the p(O) band, which results in a strong hybridization of d(Zn) and p(O) states. Therefore, the proper band structure of ZnO can be obtained by corrections applied not only to the d(Zn) electrons, but primarily to the p(O) electrons. The $+U$(O) correction directly opens the ZnO energy gap, while the $+U$(Zn) correction shifts the d(Zn) bands toward lower energies, thus reducing the $p-d$ hybridization, as illustrated in Figure 2 (b). The result of applying both corrections gives the ZnO band structure fully consistent with the experimentally observed one.

In [H4-H8], the $+U$ corrections were applied to describe pure ZnO, and in [H5-H8] also to doped TM ions. Rich experimental data for ZnO:TM allowed to verify the appropriate $+U$(TM) corrections for some TM ions, which will be discussed in section 4.3.3.

The Quantum Espresso [25] code was used in all calculations. The systems were modeled by using supercells: 16-atom cells for FeTe under pressure and 32-atom cells for FeTe:S (giving a sulfur concentration in the range of 6.25 - 25%), 96-atom cells for CuMnSb (3.1% Mn defects) and 72 and 144-atom cells for ZnO (2.8% and 1.4% TM ions). Calculations were performed on supercomputers at the Interdisciplinary Centre for Mathematical and Computational Modeling, University of Warsaw, Grants No. G46-13 and No. G16-11 [H1, H2, H4-H8], and at the Computer Center of the Tri-City Academic Computer Network, CI TASK, in Gdansk [H3].

4.3.3 Description of the results contained in works [H1-H8]

The section discuss selected properties of the considered materials, the most important results obtained in the works [H1-H8], undertaken scientific cooperation, own contribution to each of the works and the popularization at conferences and seminars.

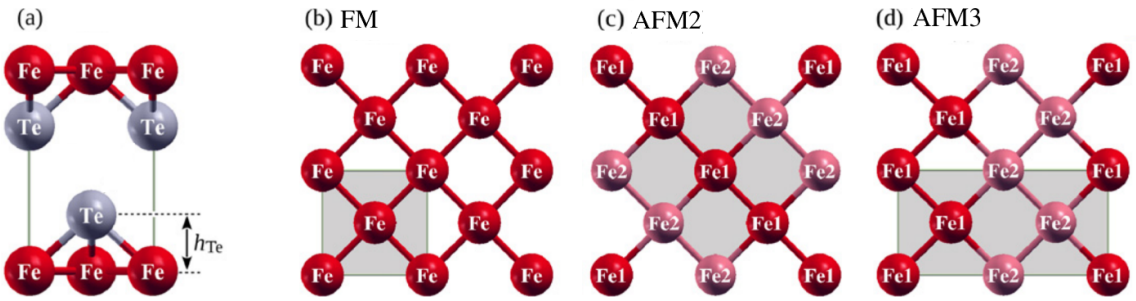

Figure 3: (a) Crystallographic structure of FeTe, with the distance between Fe and Te layers, h_{Te}, marked. Magnetic orders considered in the work and relevant for FeTe: (b) FM - ferromagnetic order, (c) AFM2 - single stripes in the [110] direction (superconducting order is observed in the experiment), (d) AFM3 - double stripes in the [100] direction. Two colors indicate two opposite directions of spins on Fe ions, additionally the magnetic unit cell in each case is marked by the shaded area.

[H1] „Magnetic phase transitions and superconductivity in strained FeTe"

The discovery of superconductivity in iron-based compounds attracted the attention of many researchers because of the relatively high critical temperatures as well as the close proximity of the superconducting and the magnetic states observed in the phase diagrams [1]. Interactions between electrons in the electron and hole bands seem to play an important role in these compounds, leading to antiferromagnetic fluctuations and the appearance of magnetic or superconducting order in the system.

The superconducting state of iron chalcogenides $FeSe_{1-x}Te_x$ is realized in a wide range of $x < 0.8$ with a maximum critical temperature $T_C = 15$ K reached for $x = 0.5$ [2]. Additionally, the critical temperature of superconducting $FeSe_{1-x}Te_x$ increases under external pressure [26]. However, the final compound, FeTe, is not superconducting and exhibits antiferromagnetic order (AFM) at low temperatures [3]. In the case of FeTe, the transition to the superconducting state is not induced even by high pressure of 19 GPa [27]. In turn, the transition from the AFM phase to the ferromagnetic phase (FM) was observed at pressure of about 2 GPa [4]. The superconducting state is obtained in epitaxial FeTe layers strained in the *ab* plane, i.e. on a $SrTiO_3$ or MgO substrate with a higher lattice constant a [6].

I undertook DFT studies of iron chalcogenides Fe(Se,Te), including magnetic phase transitions in FeTe [H1, H2], in collaboration with dr hab. Maciej Winiarski and dr hab. Małgorzata Samsel-Czekała from the Institute of Low Temperatures and Structural Research of the Polish Academy of Sciences in Wroclaw. At that time, these compounds were intensively studied experimentally in my scientific division, Division of Physics of Magnetism of the Institute of Physics of the Polish Academy of Sciences, under the management of prof. dr hab. R. Puźniak.

In paper [H1] the changes of the magnetic order of FeTe under the influence of hydrostatic and *ab*-plane biaxial pressure were considered. The calculated ground state of FeTe reproduces the experimentally observed antiferromagnetic order in the form of double-stripe spin arrangement in the [100] direction. Such order, marked as AFM3 in Figure 3 (d), is described by the propagation vector $\mathbf{q} = (\pi, 0)$. A phase transition from the antiferromagnetic state AFM3 to the ferromagnetic state was obtained under the pressure of 2 GPa, in accordance with the experiment, see Figure 4 (a). The change of the magnetic order is accompanied by a change of the crystallographic structure, i.e. the AFM3 phase is realized in a monoclinic structure, while the FM phase in a tetragonal structure. This is a phase transition of the first order, in which both the lattice constants and the volume are not continuous functions at the critical point $p = 2$ GPa.

The changes of magnetic order under *ab*-biaxial pressure are shown in Figure 4 (b). Under the compressive stress (accompanying a decrease of the crystal lattice constant a by about 3%), FeTe was obtained in a ferromagnetic state, and under the tensile stress (due to an increase in the lattice constant a by about 2%), antiferromagnetism was obtained in the form of single-stripe spins ordered in the [110] direction, see AFM2 in Figure 3 (c). Such magnetic order is described by the propagation vector $\mathbf{q}_{nest} = (\pi, \pi)$. Similar tensile stress of the lattice constant a occurs in epitaxial layers of FeTe on $SrTiO_3$ or MgO substrates, where the superconducting state, not the magnetic order, is experimentally observed. The result indicates the important role of antiferromagnetic spin fluctuations with the vector $\mathbf{q}_{nest} = (\pi, \pi)$

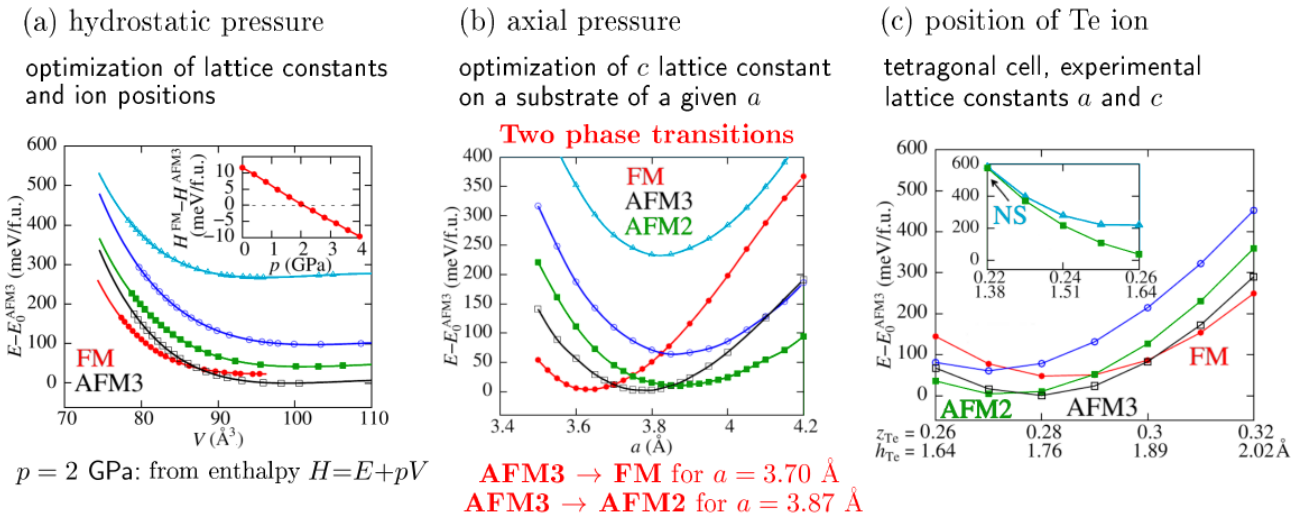

Figure 4: (a) Dependence of the total energy of FeTe (calculated relative to the equilibrium structure of AFM3) on the volume for different magnetic orders and the enthalpy difference between the AFM3 and FM states in the region the phase transition. Dependence of the total energy on (b) the lattice constant a and (c) the distance of Te ions from the iron planes h_{Te}.

in iron superconductors. In DFT calculations, where the superconducting state is not considered, the magnetically stable state is the AFM2 antiferromagnetism associated with such fluctuations. Indeed, the presence of spin fluctuations is visible in the neutron scattering spectra of superconducting iron chalcogenides [28]. The propagation vector $\mathbf{q}_{nest} = (\pi, \pi)$ is associated with a special feature of the band structure of iron chalcogenides, the so-called nesting of Fermi surface sheets, i.e. partial overlap of the electron and hole Fermi sheets after shifting by the vector $\mathbf{q}_{nest}$. Our band structure studies indicating strong nesting of Fermi surface sheets in superconducting Fe(Se,Te) [20, 21] are presented in section 7.1.

In studies under hydrostatic and axial pressure, a strong correlation between the obtained spin orders and the crystallographic structure was observed. Of particular importance is the distance of the Te ions from the iron planes, h_{Te}, see Figure 3 (a). The influence of the h_{Te} on the stabilization of a given magnetic order is illustrated in Figure 4 (c). According to our calculations, for the smallest distances h_{Te} the ground state of FeTe is the nonmagnetic, for $h_{Te} \approx 1.4$ Å the single-stripe order described by the vector $\mathbf{q}_{nest} = (\pi, \pi)$ becomes stable, for $h_{Te} \approx 1.7$ Å the double-stripe order characterized by the vector $\mathbf{q} = (\pi, 0)$ becomes stable, and for the largest distances $h_{Te} > 1.9$ Å FeTe becomes ferromagnetic.

The magnetic exchange interactions were analyzed. The intrashell exchange interaction of d(Fe) electrons gives rise to a magnetic spin moment localized on the Fe ions with the value $s_i \approx 2.5$. The interaction between the Fe ions was considered in a Heisenberg model, $H_{ex} = \sum_{n=1}^{3} J_n \sum_{i,j} s_i \cdot s_j$, including exchange integrals with nearest, second nearest, and third nearest neighbors. The obtained constants J_i showed a strong dependence on the crystallographic structure. The exchange constant J_1 describes the direct exchange between the nearest Fe ions and increases with decreasing lattice constant a (increasing h_{Te} in epitaxial layers). However, in the case of interactions mediated by Te atoms (J_2 and J_3), a decrease in the exchange constants is expected with increasing h_{Te}. The obtained dependencies of $J_2(h_{Te})$ and $J_3(h_{Te})$ did not give the reliable results. It was found that the magnetic order of FeTe depends on long-range interactions, RKKY type, which occur via conduction electrons. It was found that the magnetic ordering of FeTe is established by long-range interactions, RKKY-type, that occur via conduction electrons. In this case, not only the distances in the crystal structure are important, but also the conduction electron density.

This conclusion is consistent with the results obtained from the density of states at the Fermi level, E_F, in the paramagnetic state (i.e. from calculations without spin polarization, in which the structural parameters were taken from magnetic calculations). For h_{Te} giving the AFM2 phase, a strong decrease in the density of states at the E_F level was obtained. The observed pseudogap is typical also for other superconducting iron chalcogenides. For the h_{Te} parameters giving the AFM3 phase, the density of states increased slightly. For the largest h_{Te}, as in FM phase, the obtained density of states at the Fermi level

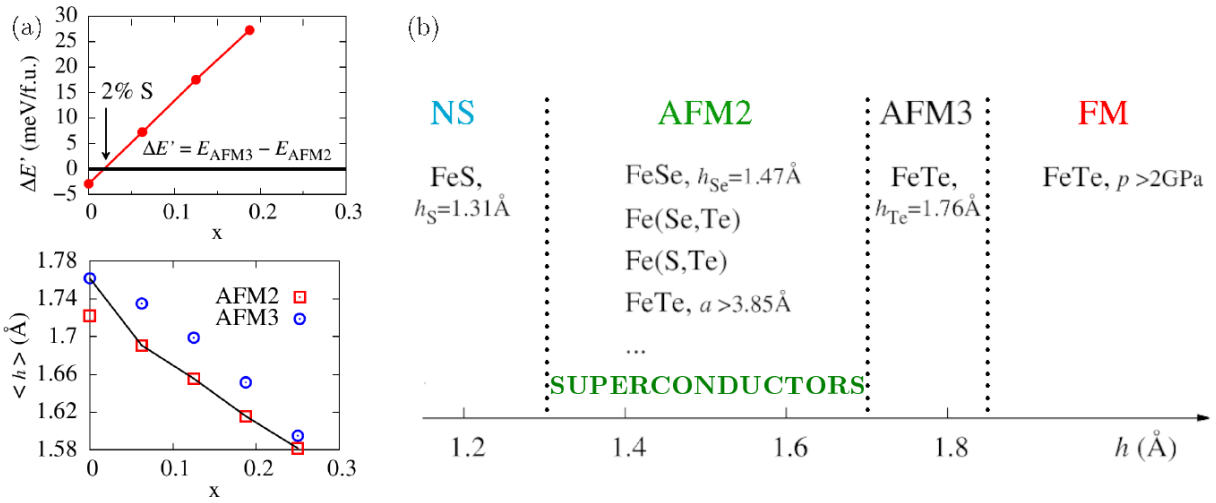

Figure 5: (a) Total energy difference between the AFM3 and AFM2 antiferromagnetic states in $FeTe_{1-x}S_x$ as a function of sulfur concentration x. (b) Dependence of the average distance of the iron chalcogenide from the iron plane $< h >$ on x. (c) Correlation between the height $< h >$ obtained for some iron chalcogenides and the calculated magnetic ground state. NS here denotes the non-magnetic state.

was more than twice as high as in the AFM states. The more metallic character of the FM phase favors long-range interactions mediated by conduction electrons.

The work [H1 was used to settle the European grant "FunDMS", managed by prof. dr hab. T. Dietl [G3], the NCN project of prof. dr hab. R. Puźniak [G5] and the NCN project of prof. dr hab. P. Bogusławski [G6].

The main achievements regarding FeTe:

- reproduction of the experimentally observed phase transition from the antiferromagnetic state, described by the vector $\mathbf{q}_{nest} = (\pi, 0)$, to the ferromagnetic state under the hydrostatic pressure of 2 GPa;
- showing that in epitaxial layers on substrates with larger lattice constant a, the calculated magnetic ground state is the antiferromagnetism associated with the nesting vector $\mathbf{q}_{nest} = (\pi, \pi)$. The obtained magnetic order is correlated with the observed superconducting state;
- indication of a strong relation between magnetic order and crystallographic structure (mainly h_{Te}).

FeTe is a highly frustrated system. Small changes in the crystallographic structure cause a change in the dominant exchange interactions and, therefore, a change in the magnetic order of Fe ions. The local magnetic moment of Fe is caused by intraatomic interactions of d(Fe) electrons, while an important channel of interatomic interactions is long-range interactions, carried by conduction electrons. They are particularly important in the ferromagnetic state, which is characterized by a high density of states at the Fermi level. The superconducting state, in turn, is observed in systems for which the calculated ground state is antiferromagnetism associated with the nesting vector $\mathbf{q}_{nest} = (\pi, \pi)$. The obtained result indicates an important role of antiferromagnetic spin fluctuations in superconducting iron chalcogenides.

Individual contribution:

The calculations in [H1] were performed by me. I am also the main author of the publication text.

[H2] „Magnetism and superconductivity of S-substituted FeTe"

The superconducting state is also observed in FeTe with Se or S ions substituted at the Te positions. $FeTe_{1-x}Se_x$ crystals are obtained in the entire x range, with the highest transition temperature to the superconducting state (T_c = 15 K) occurring for $x = 0.5$ [2]. In $FeTe_{1-x}S_x$, the superconducting state appears for $x = 0.03$ and T_c reaches 10 K [5]. In contrast to Fe(Te,Se), there is a solubility limit of S in

FeTe of 30%, caused by the large difference between the ionic radii of S and Te. Pure FeS crystallizes in a similar tetragonal structure to FeSe and FeTe [29], but the compound is neither superconducting nor magnetic.

In the work [H2], the influence of S substitution on the crystallographic, band and magnetic structure of FeTe was investigated and their relationship with the experimentally observed magnetic and superconducting ordering was determined. It was calculated that in FeTe substituted with sulfur the distance of Te ions from iron planes is almost unchanged compared to pure FeTe ($h_{Te} \approx 1.76$ A), while the S distance is similar to that obtained in pure FeS ($h_S = 1.17$ A). Thus, with increasing sulfur concentration the average distance $< h >$ decreases and for $x = 0.02$ the calculated ground state becomes the AFM2 order, see Figure 5 (a). The obtained result again indicates that in the superconducting state, antiferromagnetic spin fluctuations described by the vector $\mathbf{q}_{nest} = (\pi, \pi)$ are important. The band structure of FeTe with sulfur was also calculated to show that the presence of AFM2 fluctuations is closely related to the topology of the Fermi surface.

The correlation between the crystallographic structure and the magnetic order observed in [H1, H2] allowed generalization of the result to other iron chalcogenides. The close relationship between the average distance of chalcogenides from iron planes, $< h >$, and the calculated magnetic structure is shown in Figure 5 (b). The AFM2 magnetic order is obtained not only for FeTe epitaxial layers deposited on substrates with a sufficiently large lattice constant $a > 3.85$ A and for Fe(Te,S), but also for compounds such as FeSe and Fe(Se,Te). In the region where the calculations give the AFM2 order, chalcogenides are superconductors and in the spin excitation spectrum antiferromagnetic fluctuations of $\mathbf{q}_{nest} = (\pi, \pi)$ are observed.

The stable AFM2 state was also obtained by us in the hypothetical compounds $Ru_xFe_{1-x}Se$ and $Ru_xFe_{1-x}Te$ [22], making them potential candidates for superconductors. The calculations of the band structures of Fe(Se,Te) [20, 21] and their relation to the antiferromagnetic fluctuations described by the vector $\mathbf{q}_{nest} = (\pi, \pi)$ are presented in section 7.1.

The work [H2] was used to settle the NCN project managed by prof. dr hab. P. Bogusławski ([G6]) and the NCN project managed by prof. dr hab. R. Puźniak ([G7]).

The main achievements regarding $FeTe_{1-x}S_x$:

- showing the correlation between the crystallographic structure and the calculated magnetic order;

- showing the correlation between spin fluctuations and superconductivity.

The presence of spin fluctuations with the propagation vector $\mathbf{q}_{nest} = (\pi, \pi)$ is strongly related to the band structure and leads to the appearance of the superconducting state of iron chalcogenides.

Individual contribution:

I performed the calculations presented in [H2] and was the main author of the publication text.

The results of the work on iron chalcogenides [H1, H2] were presented at national and international conferences (listed in section 7.4: invited lecture [Z1], oral presentations [O1-O3], poster presentations [P3, P4, P6]), seminars and other presentations [S6-S9].

[H3] „Coexistence of Antiferromagnetic Cubic and Ferromagnetic Tetragonal Polymorphs in Epitaxial CuMnSb"

Heusler and half-Heusler alloys are materials with interesting physical properties from an application point of view. CuMnSb exhibits antiferromagnetic order and is a potential candidate for use in spintronics based on antiferromagnetism [7].

CuMnSb is a metal with a low density of states at the Fermi level (so-called semimetal). It crystallizes in a cubic half-Heusler structure with four fcc sublattices, one of which is empty. This structure, referred to below as the $\alpha-$CuMnSb phase, gives MnSb layers and half-filled Cu layers, as illustrated in Figure 6 (a). Responsible for magnetic properties manganese is surrounded by 12 equidistant Mn atoms, which are its second neighbors. The antiferromagnetic order, called AFM111, with alternating planes (111) of

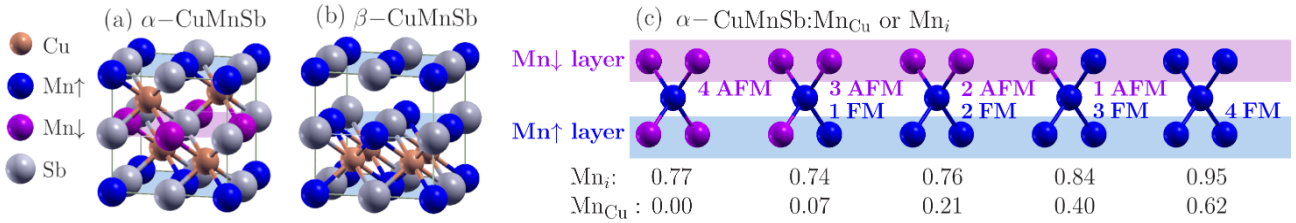

Figure 6: (a) Crystallographic structure of $\alpha-$CuMnSb and calculated antiferromagnetic order of AFM001. Spins localized on Mn are parallel in MnSb layers in (001) planes, while successive MnSb layers are antiferromagnetically coupled to each other. (b) Crystallographic structure of the ferromagnetically ordered $\beta-$CuMnSb phase. (c) Possible local spin configurations around the Mn$_i$ and Mn$_{Cu}$ defects and the formation energies of these defects given in eV.

Mn atoms with the same spin direction, has been known for years from experimental studies of neutron scattering [30]. DFT calculations also show that in the ground state $\alpha-$CuMnSb is antiferromagnetic [23, 31].

However, the theoretically determined order is different from that indicated by experiment [23]. The AFM001 order shown in Figure 6 (a) is characterized by parallel spins on Mn ions in successive (001) layers. In the work [23], it was shown that the formation energy of Mn defects is low and additional manganese ions can influence the observed magnetic order.

Theoretical studies of this antiferromagnet, conducted with prof. dr hab. Piotr Bogusławski from the Division of Theoretical Physics, Institute of Physics PAS, were undertaken in close cooperation with experimental groups: Laboratory SL1 (dr hab. P. Dłużewski and dr hab. S. Kret) and SL2 (prof. dr hab. M. Sawicki and dr K. Gas) from the IP PAS, and with the Faculty of Physics and Astronomy, Julius Maximilian University of Würzburg (dr L. Scheffler, prof. C. Gould, dr J. Kleinlein and prof. L. W. Molenkamp).

The results obtained using a transmission electron microscope indicated the presence of an additional, tetragonal crystalline phase in the CuMnSb epitaxial layers on a GaSb substrate. Magnetic studies confirmed the presence of an antiferromagnetic phase with a Néel temperature $T_N \approx 60$ K. However, they indicated an additional weak ferromagnetic contribution, which disappears at higher temperatures, about 100 K. The effective magnetic moment was determined to be $\mu_{eff} = 5.5\mu_B$, both in the ferro- and antiferromagnetic phases.

Our theoretical studies of the cubic $\alpha-$CuMnSb phase confirmed that the ground state of this alloy is AFM001, in agreement with [23]. Next, it was shown that the additional phase observed in the transmission measurements is a tetragonal phase, identified in a similar compound CuMnAs [32, 33], in which every second Cu layer is completely filled and every second completely empty. The tetragonal $\beta-$CuMnSb phase is illustrated in Figure 6 (b). The energy of the tetragonal phase is only about 0.12 eV higher than that of the cubic phase. Interestingly, its magnetic ground state is the ferromagnetic state. The obtained coexistence of the cubic antiferromagnetically ordered structure and the tetragonal ferromagnetically ordered structure explains both experimental observations and indicates that the crystallographic polymorphism in CuMnSb layers is closely related to the presence of two magnetic phases. Moreover, the calculated magnetic moment localized on Mn ions in both phases is $4.5 - 4.6\ \mu_B$, which reproduces the effective moment in the measured samples.

Exchange interactions between magnetic Mn ions are considered. The direct exchange coupling is negligibly small because of large Mn-Mn distances in the crystal, while the indirect coupling is the sum of two contributions. The nearest manganese interacts via Cu or Sb contributing to the superexchange described by the Hamiltonian in the Heisenberg model as $H_{ex} = -J_{sr}/2 \sum_{i,j} \vec{s}_i \cdot \vec{s}_j$, where only the nearest neighbor Mn are considered, and the spin value $s_i = 2.3$ is half of the calculated magnetic moment localized on Mn. The second coupling channel is the long-range RKKY interactions, mediated by free carriers.

The exchange constant $J_{sr} = -0.4$ meV was obtained by considering single spin excitations in the AFM001 magnetic phase, where long-range couplings are no important. Comparison of the energies of different magnetic orders which can be realized in the $\alpha-$CuMnSb phase within the short-range Heisenberg model leads to an antiferromagnetic coupling constant in the wide range of $J_{sr} \in (-0.6, -0.2)$ meV.

Such a divergent result indicates that the model with only short-range interactions is not suitable for metallic or semimetallic systems, such as CuMnSb, where the long-range RKKY coupling are also present.

These conclusions are confirmed by the results obtained for the $\beta-$CuMnSb phase. The band structure of the $\beta-$CuMnSb phase is similar to that of the $\alpha-$CuMnSb phase. However, the calculated density of states at the Fermi level is 3.6 times larger, which indicates a more metallic character of the $\beta-$CuMnSb phase, which favors the RKKY coupling and ferromagnetic order.

Next, the formation energies for all native point defects of cubic CuMnSb were calculated. It was shown that the defects related to antimony are of little importance, because they require high formation energies, above 1 eV. It can be assumed that the Sb sublattice is thermodynamically stable. In turn, the lowest formation energies, close to zero, were obtained for Cu vacancies, Mn vacancies and Mn_{Cu} antisites. Such defects are easy to form and can be present at high concentrations.

Of particular interest are manganese defects, since they can affect magnetic properties of CuMnSb. Anisites Mn_{Cu} and interstitials Mn_i change or induce new magnetic couplings between manganese in MnSb layers, see Figure 6 (b). Anisites are characterized by low formation energy, in particular when Mn_{Cu} couples antiferromagnetically to the nearest manganese in MnSb layers (marked as 4AFM in the figure). Such impurities prefer the ferromagnetic ordering of the nearest MnSb layers. However, low formation energy was also obtained for Mn_{Cu} defects, which couple antiferromagnetically to the three nearest manganese ions in MnSb layers (3AFM). It was proposed that Mn-related point defects induce disorder of the host AFM phase, possibly leading to formation of a spin glass.

Main Achievements for CuMnSb:

- explanation of the observed crystallographic polymorphism and two magnetic orders in CuMnSn layers;
- indication of two important channels of exchange interactions between Mn ions, i.e. short-range superexchange and long-range RKKY coupling;
- showing that the formation energy of Mn_{Cu} defect is small and dependent on the orientation of manganese spins in MnSb layers;
- showing that additional manganese ions locally change the magnetic order of neighboring MnSb layers, which can lead to the formation of spin glass, but does not explain the presence of the ferromagnetic phase in magnetization measurements (the tetragonal phase is responsible for the ferromagnetic signal).

The observed crystallographic polymorphism and the two magnetic orders are closely related, i.e. the magnetic ground state of the cubic phase is the antiferromagnetic order, while that of the tetragonal phase is the ferromagnetic order. The analysis of exchange interactions between Mn ions indicated that an important factor determining the magnetic order in CuMnSb is the density of states. The changes in the density of states at the Fermi level are responsible for the changes of the dominant magnetic coupling mechanism from antiferromagnetic superexchange in $\alpha-$CuMnSb to ferromagnetic RKKY exchange in the $\beta-$CuMnSb phase.

Individual contribution:

The paper [H3] consists of experimental measurements, theoretical calculations, and joint interpretation of results. I performed the DFT calculations and participated in the interpretation of results and text editing.

[H4] „Transition metal ions in ZnO: Effects of intrashell coulomb repulsion on electronic properties"

The doped ZnO semiconductor is the subject of intensive experimental studies on the charge and spin states of the TM, as well as optical transitions. In the context of magnetic properties, the exchange interaction between electrons on the d(TM) shell and the $s, p-d$ interactions between the magnetic moment of the TM ion and the band carriers are also important.

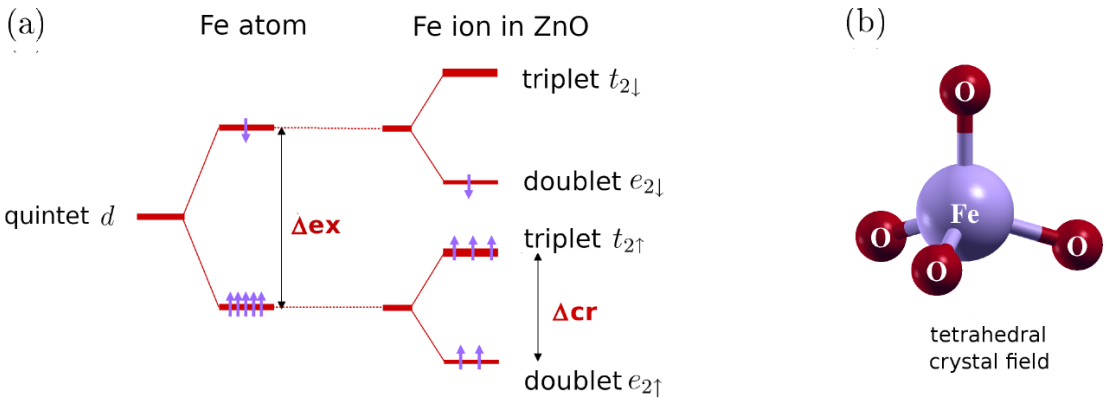

Figure 7: (a) Schematic diagram of the energy level splitting of iron Fe^{2+} due to the exchange interaction, Δex, and the crystal field, Δcr. (b) Tetrahedral environment of the iron ion in ZnO.

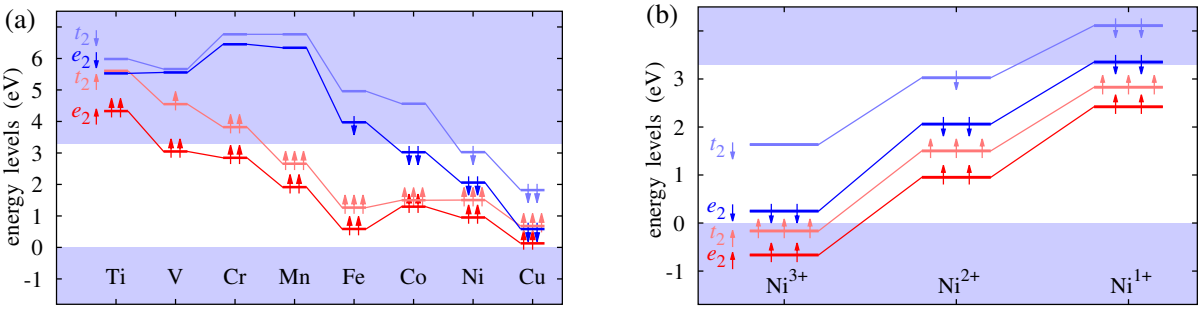

Figure 8: (a) TM levels in 2+ charge state in ZnO. (b) Ni doping levels in ZnO in different charge states.

In the work [H4], the properties of transition metal ions from Ti to Cu in ZnO were considered. The electronic structure of pure ZnO was obtained by the GGA+U method, however, the $+U$(TM) correction was not used to describe the doped ions. This approach revealed more clearly some characteristic properties related to the interaction of electrons in the d(TM) shell.

The electronic structure of the TM ion in ZnO is influenced by two effects, illustrated in Figure 7. The first one is related to the exchange splitting into states of opposite spin, Δex, according to Hundt's rule. The second one is related to the splitting of the d(TM) levels in the tetrahedral crystal field into $e_{2\sigma}$ doublets and $t_{2\sigma}$ triplets. This splitting is marked as Δcr. ZnO crystallizes in the wurtzite structure, which causes further splitting of the triplets, but this effect is neglected in the considerations. For all ions, the exchange splitting was found to be larger than the crystal field splitting, Δex > Δcr, which means that all TM ions in ZnO are in a high-spin states.

The impurity levels calculated for all considered ions in the 2+ charge state, i.e. in the charge-neutral state, are shown in Figure 8 (a). The apparent decrease in the energy of single-particle states with increasing atomic number is related to the increasing attraction of electrons by the nucleus. Qualitatively, this result is consistent with the literature [34]. Transition levels are defined as the Fermi energies relative to the top of the valence band, for which the total energies of systems with impurities in different charge states are the same. The transition levels calculated in the work indicate that most of the considered ions can occur not only in the 2+ state, but also in the 3+ or even 4+ charge state.

The paper shows two important effects related to the interaction of d(TM) electrons, i.e. to the intrashell exchange interaction and to the intrashell Coulomb interaction. These effects are also important in other works on doped ZnO semiconductor [H5-H8].

First, the spin splitting is qualitatively well described by the Heisenberg model, $H = -2J\sum_{i,j>i}\vec{s}_i\cdot\vec{s}_j$, where the summation goes over the one electron states with the spin $\vec{s}_i$. In Figure 8 (a), one can observe increase of the spin splitting for 2+ ions, comparable for e_2 doublets and t_2 triplets, going from Ti ($\Delta\text{ex} \sim 1\ eV$) to Mn ($\Delta\text{ex} \sim 5\ eV$). Then, this splitting decreases with increasing electron number $d\downarrow$,

i.e. from Mn to Cu, again to the value $\Delta \text{ex} \sim 1\ eV$. This almost linear dependence of the splitting on the magnetic moment located on the dopant allows estimating the exchange integral to $J \approx 1$ eV for all ions. This model is valid for TM ions in other charge states, since the largest splitting for dopants in the 3+ state is observed for Fe.

Secondly, the position of impurity levels show a strong dependence on occupancy. An example dependence of impurity levels on the charge state for Ni is shown in Figure 8 (b). It can be observed that with increasing number of d electrons on TM ion, the single-particle energy levels also increase. This increase is large, in the case of Ni it is ~ 2 eV, i.e. it is comparable to the spin splitting and significantly exceeds the splitting associated with the crystal field. This is an effect of a strong, intra-shell Coulomb repulsion. The more electrons occupy d(TM) shell, the stronger the repulsion between them, which results in the increase of dopant levels, $e_{2\sigma}$ and $t_{2\sigma}$. This property is characteristic of all TM ions. The intrashell Coulomb interaction is responsible, among others, for the instability of Mn^{3+} ions [H6] and the charge state-dependent $s, p-d$ exchange interactions [H8], which is discussed in the further part of the scientific achievement.

The work [H4] was done in cooperation with prof. dr hab. P. Bogusławski. It was used to settle the project I managed, financed by the National Science Center [GW].

The main achievements regarding doped ZnO presented in this paper:

- illustration (qualitative) of the changes in TM impurity levels in the 2+ state with increasing atomic number;
- indication of the strong, intrashell Coulomb interaction for d(TM) electrons, visible as an increase in the energy of the TM levels with increasing occupancy;
- analysis of the exchange interactions for d(TM) electrons, consistent with the Heisenberg model, and estimation of the exchange constant to $J \approx 1$ eV for all Tms;
- calculation of transition levels, showing that TM ions in ZnO can occur in different charge states (most ions in the 2+ and 3+ states).

For TM ions in ZnO, the important interactions that affect the position of the impurity levels are the interaction with the crystal field (with p(O) electrons in the tetrahedral environment) and intrashell interactions, i.e. exchange and Coulomb interactions. The intrashell interactions are included in the LDA/GGA approximation. Adding the $+U$(TM) corrections, shown in works [H5-H8], affects the positions of the dopant levels, but does not change the trend shown in Figure 8 (a) and (b).

Individual contribution:

In the paper [H4] I performed DFT calculations and calculations related to the exchange integral and transition levels between charge states. I participated in the analysis of the results and writing the text of publication.

[H5] „Calculated optical properties of Co in ZnO: internal and ionization transitions"

Doping ZnO semiconductor with Co ions results in the appearance of a series of optical transitions, which have been the subject of experimental [35, 36, 37, 38] and theoretical [39] studies for years. Ionization transitions, associated with the change of the Co charge state, were observed in the luminescence and absorption spectra, shifted relative to each other, in accordance with the Franck-Condon principle. Next, the narrow internal transition $d \rightarrow d^*$, giving the same line in both spectra, is characterized by a weak fine splitting, associated with the crystal field and spin-orbit interaction. The internal transition can be easily distinguished from ionization transitions in transport measurements, because it does not generate additional carriers and therefore does not give photocurrent [37, 38]. Finally, interband transitions are also observed, analogous to pure ZnO, and provide information on the change of the ZnO energy gap due to Co doping [36, 38].

In paper [H5], all transitions were reproduced to an accuracy of 0.1-0.2 eV using a single correction $U(\text{Co}) = 3$ eV. From the linear response theory [18], a similar value of the parameter $U(\text{Co}) = 3.4$ eV was obtained. The correction affects the position of the Co levels, according to the equation (6). Compared

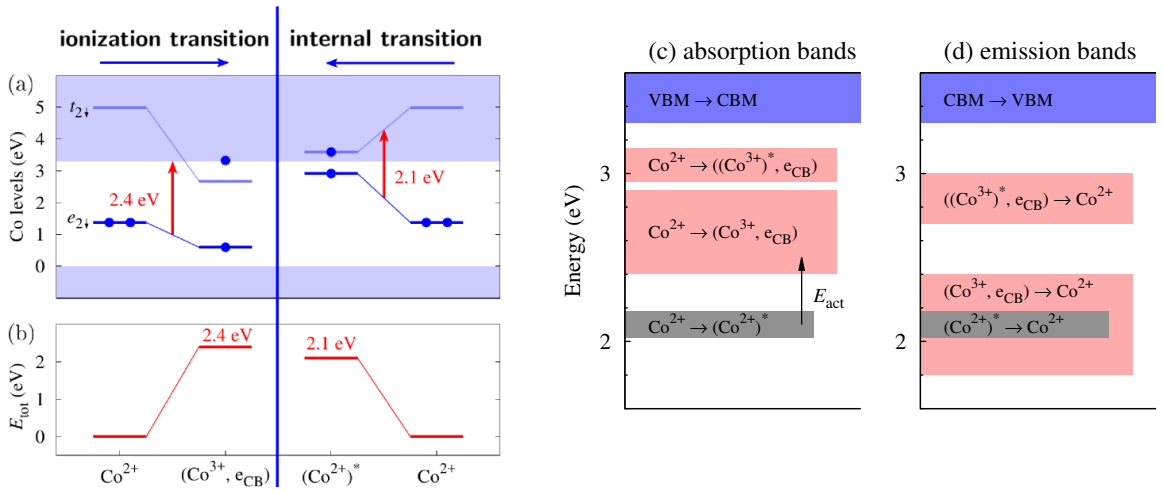

Figure 9: (a) Changes of Kohm-Sham levels and (b) changes of total energy of the system at the $Co^{2+} \rightarrow Co^{3+}$ ionization transition and $Co^{2+} \rightarrow (Co^{2+})^*$ internal transition. Only the $e_{2\downarrow}$ and $t_{2\downarrow}$ levels are shown, the occupation of which changes. Calculated (c) absorption and (d) emission bands in ZnO:Co.

to Figure 8 (a), for Co^{2+} with occupation $(e^2_{2\uparrow}t^3_{2\uparrow}, e^2_{2\downarrow}t^0_{2\downarrow})$, the fully occupied levels, $e_{2\uparrow}$, $t_{2\uparrow}$ and $e_{2\downarrow}$, are shifted toward lower energies, while the empty level $t_{2\downarrow}$ is shifted toward higher energies.

The obtained results allowed us to observe changes in the position of Co levels in optical transitions. Intrashell Coulomb and exchange interactions, discussed in [H4], strongly affect the position of impurity levels in ionization transitions since the charge state of Co changes. In turn, during internal transitions, the shift of TM levels is caused by the applied $+U$(Co) correction. In such a $d \rightarrow d^*$ transition, the occupation of Co^{2+} levels changes (one electron from $e_{2\downarrow}$ moves to $t_{2\downarrow}$), the $+U$ term shifts up the level with lower occupation, and shifts down the level with higher occupation. The effect of both mechanisms is presented in Figure 9 (a).

The influence of intrashell interactions on dopant levels indicates that their knowledge in the charge neutral state, the 2+ state, does not allow for the correct determination of optical transitions. It has been shown that transition energies can be calculated from the difference in total energy between the initial and final states, see Figure 9 (b). An alternative method is to use Janak's theorem [13] and calculate the energy of any transition from the averaged single-particle levels (such a method is illustrated by the arrows in Figure 9 (a)). In the case of ionization transitions, knowledge of transition levels can be used. The energy distance between the (2+/1+) transition level and the top of the valence band gives the transition energy $Co^{2+} \rightarrow Co^{1+}$, and the distance between the (3+/2+) transition level and the bottom of the conduction band gives the ionization energy $Co^{2+} \rightarrow Co^{3+}$. It was shown that all methods lead to consistent results.

Obtaining transition energies consistent with experiment allowed their following interpretation:

1. The ionization transition $Co^{2+} \rightarrow Co^{3+}$ with energy of 2.4 eV (zero-phonon line) creates an absorption band at energies 2.4-2.9 eV, and in the emission band at 1.8-2.4 eV.

2. The ionization transition $Co^{2+} \rightarrow (Co^{3+})^*$, i.e. the transition to the excited $(Co^{3+})^*$ state with occupation $(e^2_{2\uparrow}t^2_{2\uparrow}, e^2_{2\downarrow}t^0_{2\downarrow})$, gives absorption band at 3.0-3.1 eV and luminescence band at 2.7-3.0 eV. This transition was proposed instead of the $Co^{2+} \rightarrow Co^{1+}$ transition suggested earlier in the literature [38]. According to our calculations, the excitation of Co to the 1+ state would require an energy above 4 eV, much higher than the energy of excitation of an electron from the bottom of the valence band to the top of the conduction band.

3. The internal transition $Co^{2+} \rightarrow (Co^{2+})^*$, where the occupation of Co levels changes from $(e^2_{2\uparrow}t^3_{2\uparrow}e^2_{2\downarrow}t^0_{2\downarrow})$ to $(e^2_{2\uparrow}t^3_{2\uparrow}e^1_{2\downarrow}t^1_{2\downarrow})$ forms a narrow band around the energy of 2.1 eV.

The linear widening of the energy gap in doped ZnO is also shown. The gap changes according to the equation $E_{gap}(x) = E(0) + bx$, where $E(0) = 3.3$ eV is the gap of pure ZnO, the fitted coefficient $b = 1.9$ eV, and x is the Co concentration in a wide range up to 12.5%. The obtained dependence is in good agreement with experiment [38]. The final result of the work of [H5] are the calculated absorption and emission band energies presented in Figure 9 (c) and (d).

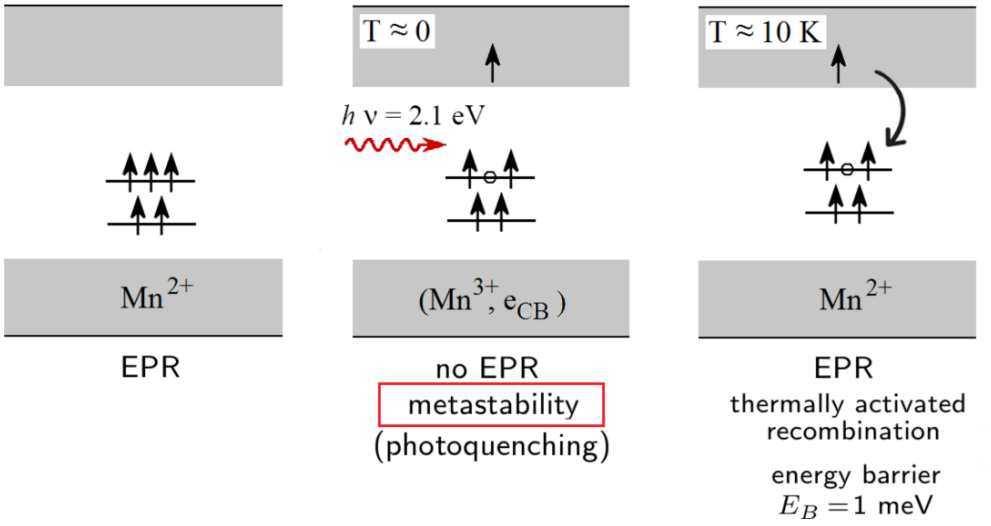

Figure 10: Scheme of the observation of the metastability of the Mn^{3+} ion in ZnO in EPR measurements.

The work [H5] was done in cooperation with prof. dr hab. P. Bogusławski. It was used to settle the project I managed, financed by the National Science Center [GW].

Main achievements regarding Co-doped ZnO:

- reconstruction of experimental absorption and emission spectra with an accuracy of 0.2 eV;
- new interpretation of the band observed around 3 eV;
- indication of the strong Coulomb interaction and the $+U$(TM) correction as factors strongly changing the positions of the Kohn-Sham levels;
- determination of the $+U$(Co) correction.

In the context of electron-electron interactions, the intrashell Coulomb repulsion (related to the dependence of levels on the charge state of Co) and the exchange interaction (related to the splitting of states with opposite spin) play an important role, which was shown in [H4]. The necessity of adding the $+U$(Co) correction indicates that the exchange-correlation interactions included in the standard LDA/GGA approximation are insufficient to describe TM ions in ZnO.

Individual contribution:

The calculations presented in the work [H5] were performed by me, the work was written and interpreted together with prof. dr hab. Piotr Bogusławski.

[H6] „Metastability of Mn^{3+} in ZnO driven by strong d(Mn) intrashell Coulomb repulsion: experiment and theory"

Manganese dopant in ZnO has been the subject of many experimental works [37, 40, 41]. In particular, the ionization transition $Mn^{2+} \rightarrow (Mn^{3+}, e_{CB})$, in which Mn^{2+} releases an electron to the conduction bands (CB) and goes to a 3+ charge state, has been observed. The absorption threshold of the ionization transition (zero-phonon energy) is 2.1 eV.

The Mn dopant was studied experimentally at IP PAS under management of prof. dr hab. Andrzej Suchocki from the ON4 division in ZnO:Mn crystals grown in the ON1 division (prof. dr hab. A. Mycielski, dr P. Skupiński and dr hab. K. Grasza). EPR measurements performed by dr hab. Hanna Przybylińska allowed to observe photoquenching of Mn^{2+} signal at low temperatures under illumination with light of about 600 nm ($\sim$ 2 eV). This effect is related to the photoionization transition of Mn ions from the 2+ to 3+ state. Photoquenching indicates that the excited state of Mn is metastable. Electron capture by Mn and recombination to the 2+ state are thermally activated. Based on the experimental data, the energy

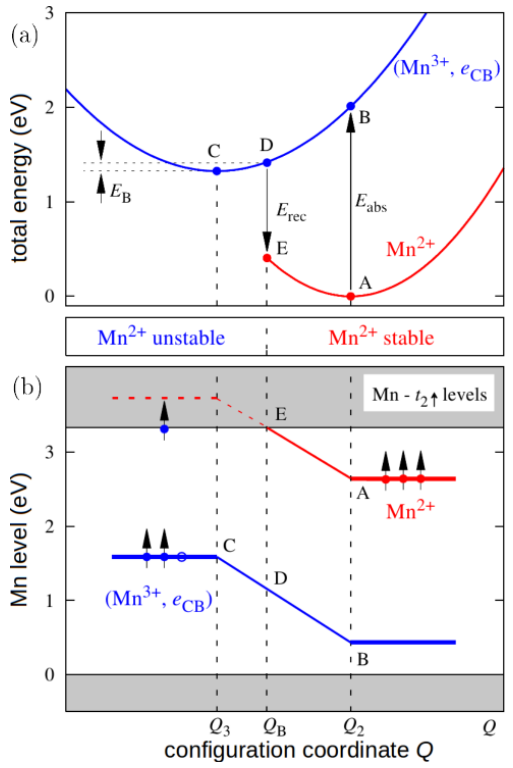

The absorption-recombination cycle in 5 steps:

1. A→B: absorption at configuration Q_2
   $E_{abs} = 2.0$ eV $\quad (E_{abs} = 2.4$ eV$)$
2. B→C: relaxation (Mn^{3+}, e_{CB}) to Q_3
   $E_{relax} = -0.6$ eV $\quad (E_{relax} = -0.4$ eV$)$
   The final state is metastable
3. C→D: a thermally driven transition to the barrier configuration Q_B
   $E_B = 60$ meV $\quad (E_B = 1$ meV$)$
4. D→E: recombination to Mn^{2+} at Q_B
5. E→A: relaxation of Mn^{2+} to Q_2

metastability driven by intra-shell Coulomb repulsion + lattice relaxation

Figure 11: Dependence of (a) the total energy and (b) the $t_{2\uparrow}$ levels of manganese in the 2+ and 3+ states on configuration coordinate Q and explanation of the mechanism of Mn^{3+} metastability. Energies calculated for the subsequent transitions are shown for $U(\mathrm{Mn}) = 0$ and (in parentheses) for $U(\mathrm{Mn}) = 1.5$ eV.

barrier for recombination was estimated to be about 1 meV. Schematically, the changes of Mn charge state in the subsequent stages of photo-EPR measurements are illustrated in Figure 10.

The calculations explained the experiment. A mechanism leading to the metastability of Mn^{3+} was proposed. The observed metastability is the result of two effects. First, the metastability of Mn^{3+} is related to the strong Coulomb interaction between d(Mn) electrons [H4, H5]. The second mechanism is related to lattice relaxation. The equilibrium bond lengths of Mn^{3+} with the nearest oxygen atoms, defined by the configuration coordinate Q, are shorter than for Mn^{2+}. In turn, for a fixed Q configuration, the Mn^{2+} levels lie higher than the corresponding levels for the Mn^{3+} ion. The most important level here is $t_{2\uparrow}$, the occupancy of which is changing.

Figure 11 explains the absorption and recombination process and the resulting mechanism of Mn^{3+} metastability. Part (a) shows the dependence of the total energy for Mn^{2+} and Mn^{3+} in ZnO at the configuration coordinate Q, while part (b) shows the changes in the triplet position $t_{2\uparrow}$ for both these ions. Mn^{2+} at the equilibrium configuration Q_2 gives the level $t_{2\uparrow}$ in the energy gap. Its ionization to Mn^{3+} requires the energy E_{abs}. It turns out that Mn^{3+} at the Q_2 configuration has a triplet level located 2 eV lower than Mn^{2+}. During relaxation to the equilibrium configuration Q_3, the Mn-O bond lengths shorten and the impurity levels shift to energies higher by ~ 1 eV. At such a configuration, the $t_{2\uparrow}$ level for Mn^{2+} would be in the conduction band. It would be energetically unfavorable and lead to autoionization of the electron from the impurity level to the bottom of the conduction band (and thus to the (Mn^{3+}, e_{CB}) state). Therefore, Mn^{2+} cannot be stable at the Q_3 configuration. The system requires energy to excite Mn to the configuration Q_B, where the triplet state of Mn^{2+} is located in the energy gap. Then, recombination $(Mn^{3+}, e_{CB}) \rightarrow Mn^{2+}$ proceeds in the standard way and the lattice relaxes from barrier configuration Q_B to the equilibrium configuration Q_2.

Comparison of our results to experimental data allowed us to fit the correction $+U$(Mn). Using $U(\mathrm{Mn}) = 1.5$ eV correctly reproduces the Mn ionization energy (both in the vertical transition, ~ 2.4 eV, and the zero-phonon line, ~ 2.0 eV) and gives the metastability of Mn^{3+} under illumination. It also allowed us to estimate the small energy barrier for recombination, ~ 1 meV, consistent with experiment.

The work [H6] was used to settle the NCN project, managed by prof. dr hab. P. Bogusławski [G6].

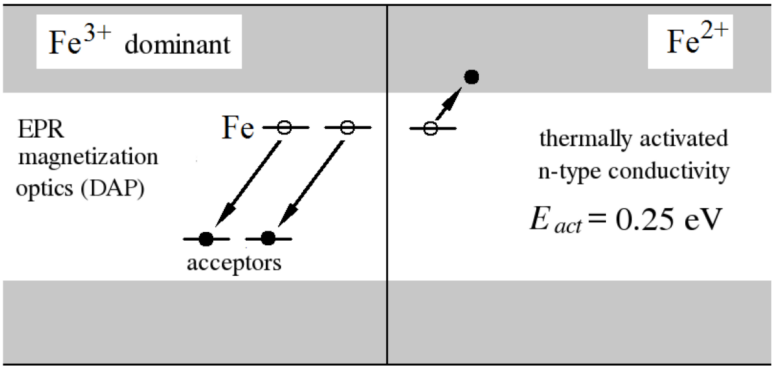

Figure 12: Explanation of (i) dominant contribution of Fe in the 3+ charge state in ZnO by the presence of acceptor levels in the gap and (ii) thermally activated n-type conductivity by $Fe^{2+} \rightarrow Fe^{3+}$ ionization.

Main achievements concerning Mn ions in ZnO:

- explanation of metastability of Mn^{3+} by the strong Coulomb interaction between d(Mn) electrons and by local lattice relaxation around the impurity. The Coulomb-induced dependence of the impurity energy levels on its charge state is a new, previously unconsidered mechanism of metastability;
- fitting the correction $+U$(Mn) to experimental data.

The intra-shell Coulomb repulsion for d(Mn) electrons and the $+U$ correction strongly influence the impurity levels. Additionally, effects related to lattice relaxation indicate the antibonding nature of the wave functions, i.e. shortening of the Mn-O bonds results in a stronger Coulomb repulsion between electrons on both ions and an increase in single-particle levels. The antibonding nature of the wave functions for selected TM ions was illustrated in publications [H7] and [H8].

Individual contribution:

The paper [H6] consists of an experimental and theoretical part. The theoretical part was developed by me and prof. dr hab. P. Bogusławski. I was responsible for the calculation, as well as joint interpretation of results and text editing.

[H7] „Fe dopant in ZnO: 2+ versus 3+ valency and ion-carrier $s,p-d$ exchange interaction"

In II-VI semiconductors, the charge-neutral state of TM ions is the 2+ state. However, the valency of these ions may be different due to the presence of unintentional defects or impurities that introduce additional carriers in the crystal, thus influencing the position of the Fermi level. The valence state of Fe dopants in ZnO has been the subject of many experimental studies that detected the presence of both 2+ and 3+ ions [42] or exclusively 3+ ions [43].

In the work [H7], the Fe dopant in ZnO was studied in order to determine its charge state and interaction with band carriers. The research was undertaken in cooperation with the Faculty of Physics of the University of Warsaw (prof. dr hab. M. Nawrocki, prof. dr hab. A. Twardowski, dr hab. A. Drabińska, dr hab. G. Kowalski, dr hab. J. Szczytko, dr hab. W. Pacuski, dr hab. J. Suffczyński, dr M. Tokarczyk, mgr A. Gardias, mgr J. Papierska, mgr K. Sawicki), the Department of Solid State Physics in Giza (prof. M. Boshta, prof. M. M. Gomaa) and the University of Versailles St-Quentin in Yvelines-CNRS (dr E. Chikoidze and prof. Y. Dumont) and employees of our institute, IP PAS (dr hab. H. Przybylińska and dr hab. B. Witkowski). The theoretical part of the work was developed by me and prof. dr hab. P. Bogusławski.

Comprehensive experimental studies included EPR, magnetization, optical and transport measurements. Magnetooptic measurements indicated a high concentration of Fe^{3+} ions in the tested samples. In turn, transport measurements showed thermally activated n type conductivity.

The parameter $+U(\mathrm{Fe}) = 4$ eV used in DFT calculations reproduced the measured activation energy $E_{act} = 0.25$ eV, which allowed to reconcile and interpret the experimental and theoretical results. According to the calculations, the stable state in ideal ZnO is the Fe^{2+} state. However, the high position of the transition level (3+/2+) makes that such iron can be easily compensated by unintended acceptors, probably zinc vacancies [44]. In turn, the part of ions that remains in the 2+ state at low temperatures is thermally activated (ionized also to the 3+ state), giving the n type conductivity. A schematic illustration of the conclusions drawn from the measurements and calculations is presented in Figure 12.

MCD (*Magnetic Circular Dichroism*) and magnetophotoluminescence measurements indicated significant $s, p-d$ exchange interactions between band carriers and d(Fe) electrons. The exchange constants for these interactions were calculated and the mechanism of $s-d$ and $p-d$ interactions was illustrated. At the same time, it drew our attention to the relevance of this type of research and prompted us to further consider $s, p-d$ interactions for a larger group of TM ions in ZnO. The research was undertaken in the work [H8], the results of which is discussed and generalized in the next point of the scientific achievement.

The work [H7] was used to settle the NCN project, managed by prof. dr hab. P. Bogusławski [G6].

Main achievements regarding Fe ions in ZnO:

- obtaining the levels of Fe^{2+} and Fe^{3+} for which the thermally activated ionization energy is consistent with experiment;
- explaining the coexistence of Fe^{2+} and Fe^{3+} ions in the tested ZnO samples;
- calculating the exchange constants for the $s, p-d$ coupling;
- determining the $+U$(Fe) correction.

As for other TM ions [H4-H6], the properties of Fe ion in ZnO are significantly influenced by the exchange interaction of d(Fe) electron, which spin-split Fe levels, and by the intrashell Coulomb interaction, which changes Fe impurity levels with the change of the charge state. The $+U$(Fe) correction must be taken into account to describe this ion. Furthermore, the visible splitting of the ZnO band states and the calculated exchange constants indicate a strong $s, p-d$ coupling between the Fe magnetic moment and the band carriers, electrons in the conduction band and holes in the valence band. This coupling is dependent on the Fe charge state.

Individual contribution:

The paper [H7] also consists of an experimental and theoretical part. The theoretical part was developed by me and prof. dr hab. P. Bogusławski. I was responsible for the calculations, the interpretation of the results was consulted with the experimental groups.

[H8] „Theory of the sp - d coupling of transition metal impurities with free carriers in ZnO"

For years, II-VI and III-V semiconductors doped with transition metals have been the subject of extensive experimental [36, 41, 45, 46, 47] and theoretical [48, 49, 50] studies concerning the $s, p-d$ interaction between the magnetic moment localized on transition metal dopant and the spins of band carriers. This coupling is one of the most important characteristics of dilute magnetic semiconductors considered in spintronic applications [9]. In the paper [H8], exchange constants of $s, p-d$ coupling for TM dopants ranging from Ti to Cu in ZnO were obtained within the density functional theory.

The $+U(TM)$ correction, determined for some TM ions in [H5-H7], was added to the description of electron interactions on dopant ions. It was shown that most TM ions in ZnO can exist in two charge states, 2+ and 3+. The exceptions are Ti, which can exist only in 4+ charge state (so it is a nonmagnetic dopant), and V, which can exist in 3+ or higher charge state. Knowledge of the splitting of band states, induced by the presence of a magnetic dopants, allowed for a detailed analysis of the $s, p-d$ interactions and the calculation of the exchange constants, $N_0\alpha$ and $N_0\beta$.

The exchange constant $N_0\alpha$ is defined for interactions between d(TM) electrons and s electrons forming the conduction band bottom ($s-d$ interaction), while the constant $N_0\beta$ defines the interaction

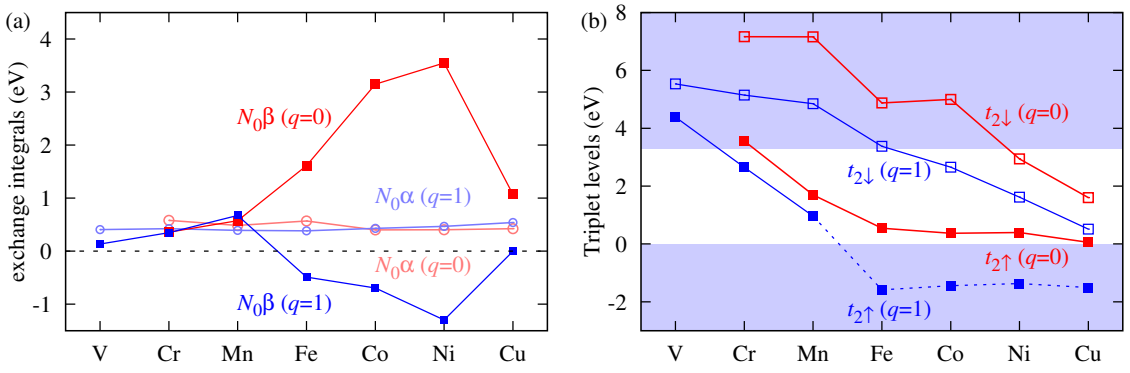

Figure 13: (a) The exchange constants $N_0\alpha$ and $N_0\beta$ and (b) the position of $t_{2\sigma}$ triplet levels for TM ions in charge states 2+ ($q = 0$) and 3+ ($q = 1$). The triplet levels degenerate with the valence band are shown only schematically.

with p holes in the valence band top ($p - d$ interaction). The splitting of the conduction band bottom, $\Delta\epsilon_c$, and the valence band top, $\Delta\epsilon_v$, in the range of small impurity concentrations x, for which $\Delta\epsilon_{c/v} \sim x$, allowed us to determine both constants:

$$N_0\alpha = \Delta\epsilon_c/(x < S >); \qquad N_0\beta = \Delta\epsilon_v/(x < S >), \tag{8}$$

where $< S >= (N_\uparrow - N_\downarrow)/2$ is related to the magnetic moment of the impurity, i.e., the difference in the occupation of the impurity states by electrons with opposite spins, $N_\uparrow$ and $N_\downarrow$.

The main result of the work is shown in Figure 13 (a). It shows the exchange constants $N_0\alpha$ and $N_0\beta$ for TM ions from V to Cu in ZnO for charge states 2+ and 3+ (for nonmagnetic Ti by definition $N_0\alpha = 0$ and $N_0\beta = 0$).

It was shown that the $s - d$ interaction is always ferromagnetic, and the exchange constant is almost independent of the TM ion and its charge state, $N_0\alpha \approx 0.5$ eV. It is related to direct exchange on the TM ion as well as on the nearest oxygen ions. The first contribution has been known for a long time [51], it is an intraatomic effect, in which d(TM) electrons induce spin polarization of s(TM) electrons forming the conduction band. This effect is therefore related to the overlapping of wave functions on the impurity. The second contribution is a new effect, related to the spin polarization of s(O) electrons of the valence band in the vicinity of the magnetic impurity. It is the result of the p(O) $- d$(TM) hybridization, which leads to weak magnetization of oxygen ions. Consequently, it is also an intraatomic effect, in which spin-polarized p(O) electrons lead to polarization of s(O) electrons. This new $s - d$ coupling channel contributes about 30% to the spin splitting of the conduction band.

In turn, the exchange constant $N_0\beta$ for the $p-d$ coupling depends on both the dopant and its charge state, see Figure 13 (a). Going from V to Ni, the value of $|N_0\beta|$ strongly increases. Furthermore, for Fe, Co and Ni, the sign of $N_0\beta$ depends on the charge state, i.e. the constant $N_0\beta$ is positive indicating the ferromagnetic $p-d$ coupling for charge neutral TM^{2+} ions, $N_0\beta$ is negative and the $p-d$ coupling is antiferromagnetic for TM^{3+} ions. Moreover, the exchange constant $N_0\beta$ may be different for light holes and heavy holes (this is not visible in the figure, which shows the average value of $N_0\beta$). For the Cu ion, which induces strong spin splitting of the bands, the constant $N_0\beta$ for light holes and heavy holes has the opposite sign (and thus the average value of $N_0\beta$ is small).

The $p - d$ coupling is described by the Anderson model, in which the splitting of the valence band top, $\Delta\varepsilon_v \sim N_0\beta$, is related to the spin-dependent hybridization $V_{hop,\sigma}$ between d(TM) and p(O) states and the relative distance of the triplet levels $t_{2\sigma}$ from the valence band top [50]:

$$\Delta\varepsilon_v = \frac{1}{2}\left(\frac{|V_{hop,\uparrow}|^2}{\varepsilon(t^0_{2\uparrow}) - \varepsilon^0_v} - \frac{|V_{hop,\downarrow}|^2}{\varepsilon(t^0_{2\downarrow}) - \varepsilon^0_v}\right), \tag{9}$$

where the "0" subscripts at the energies refer to states not perturbed by the interaction.

The wave functions squared of the valence band top, shown in Figure 14 (a) for ZnO:Co, indicate that hybridization between the p(O) and d(TM) states is indeed spin dependent. Energies of the TM

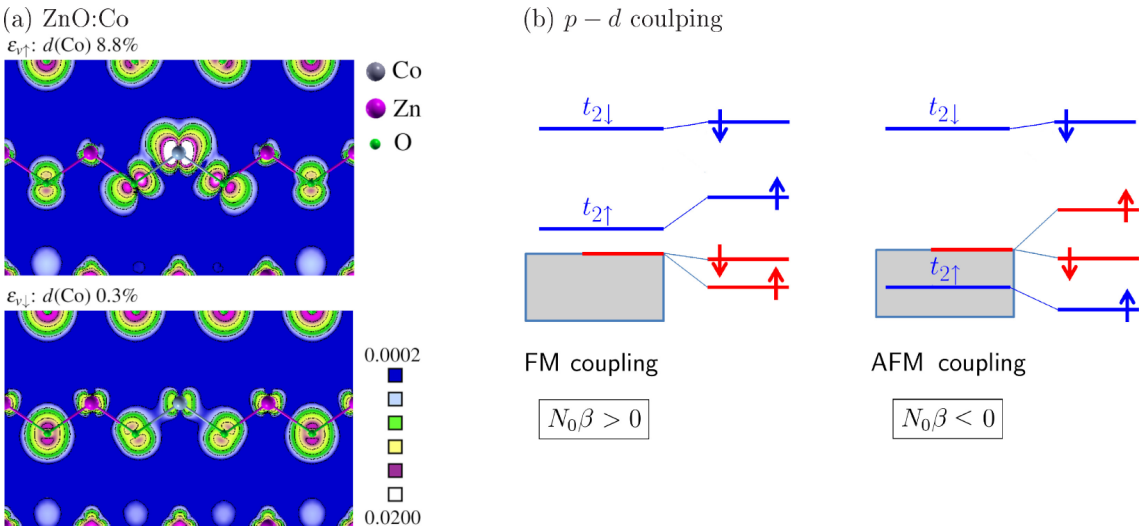

Figure 14: (a) The wave functions squared of the top of the valence band (sum over p states) of ZnO doped by Co^{2+} with the contribution from d(Co) electrons shown. (b) Dependence of $sp-d$ exchange coupling on the position of the triplet levels $t_{2\sigma}$ relative to the valence band.

triplet levels are shown in Figure 13 (b). Equation (9) together with the figure qualitatively explain the calculated characteristics of $N_0\beta$ in terms of the tryplet energy levels relative to the valence band. The $t_{2\downarrow}$ states for all considered TM impurities in ZnO lie above the valence band giving an antiferromagnetic contribution to the $p-d$ coupling. The $t_{2\uparrow}$ levels lie much closer to the valence band than $t_{2\downarrow}$, so they determine the band splitting and the sign of the $N_0\beta$ exchange constant. For all TM^{2+} ions, $t_{2\uparrow}$ triplets are located above the valence bandey giving ferromagnetic coupling. In the case of Fe, Co, and Ni in 3+ charge state, their triplet levels are degenerate with the valence band and the $p-d$ coupling is antiferromagnetic. The mechanism of spin splitting of the valence band top is illustrated in Figure 14 (b).

The theoretical results obtained for Ti, V, Cr and Mn are in good agreement with the experiment [45, 46]. So far, the analysis of experimental data [47] and theoretical models [49] for most ions assumed that their impurity states are degenerate with the valence band, as is the case for CdTe:TM, which results in antiferromagnetic $p-d$ coupling. In the case of Fe, Co and Ni, a reliable comparison of the obtained results requires an experimental determination of the charge states of these ions in ZnO.

The work [H8] was done in cooperation with prof. dr hab. Piotr Bogusławski. It was used to settle a grant financed by the National Science Center and managed by me [GW].

Main achievements of the work:

- determination of possible charge states of the considered TM ions in ZnO;
- calculation of the exchange constants $N_0\alpha$ and $N_0\beta$ for TM ions in the 2+ and 3+ charge states;
- indication of a new channel contributing to the $s-d$ coupling, which is the $p-d$ hybridization;
- explanation and illustration of the mechanism of the $p-d$ exchange coupling.

The work [H8] discuss all interactions for d(TM) electrons in ZnO presented in [H4-H7], i.e. the interaction with the crystal field and intrashell interactions as Coulomb repulsion and exchange interaction.

The paper also points to further interactions for d(TM) electrons. The first one, the $s-d$ coupling, is also an intraatomic effect (but not an intrashell effect) related to the overlap of wave functions. It causes the spin polarization of s(TM) electrons and gives the main contribution to spin splitting of the conduction band bottom. The second interaction is related to the hybridization between the d(TM) dopant states and the p(O) band states. This hybridization is effectively described by the $p-d$ exchange, called kinetic exchange. It causes spin polarization of p(O) orbitals around the TM dopant and splits the valence band states.

Individual contribution:

The DFT calculations presented in the paper [H8] were performed by me, the results were discussed and the paper was written together with prof. dr hab. Piotr Bogusławski.

The results of the work on ZnO doped with TM ions [H4-H8] were presented at conferences as invited lectures [Z2], oral [O4-O6] and poster presentations [P8, P11, P13-P17], as well as at seminars and other presentations [S10-S17].

4.3.4 Summary

In the series of works [H1-H8] constituting this scientific achievement, electron-electron interactions in systems containing transition metal ions were analyzed. In particular, semimetallic FeTe (in which Fe ions are components of the compound) and CuMnSb (in which TM ions are components of the compound, as well as native point defects) and semiconducting ZnO (in which TMs are dopants) were considered.

Transition metal ions are characterized by the presence of a partially filled $3d$ shell. It retains its localized character also in the compounds under consideration. And, unlike the atomic valence shells s and p, it creates narrow energy bands or localized states. The degree of localization of wave functions influences the electron-electron interaction. In general, in the discussion of interaction mechanisms and their influence on electronic structure, the simple Coulomb interaction (analog of the classical interaction) and the exchange interaction are considered separately.

Strong localization of the wave function leads to strong electron-electron coupling in the case of intrashell interaction between d(TM) electrons. The exchange channel causes the existence of a nonzero magnetic moment of the TM ion in the crystal. On the other hand, the Coulomb interaction causes a strong dependence of the energy of the TM ion levels on its charge state. In the considered ZnO semiconductor, the energies of the impurity TM levels can change by about 1 eV, which is comparable to the energy of the band gap.

The second aspect of electron-electron interaction is the interaction between d(TM) electrons and band electrons, i.e. $s-d$ and $p-d$ coupling, described by two exchange constants, $N_0\alpha$ (with the conduction band) and $N_0\beta$ (with the valence band), respectively. The analysis carried out showed that the source of the $N_0\beta$ constant is a mechanism resulting from the hybridization of d(TM) orbitals with p orbitals forming the top of the valence band. This hybridization depends on the position of d(TM) levels relative to the top of the valence band. As shown in [H7, H8], this model describes well the $p-d$ coupling in doped ZnO. The new aspect, in relation to the published works, is (i) showing the strong dependence of the exchange constant $N_0\beta$ on the charge state of the TM ion, and (ii) the possibility of changing the sign of $N_0\beta$, i.e. changing the nature of the interaction from ferromagnetic to antiferromagnetic. Both effects are the result of strong intrashell Coulomb repulsion of d(TM) electrons. In turn, the constant $N_0\alpha$ has so far been interpreted as the result of interaction between d(TM) states and s conduction states. As shown in [H8], a significant contribution, of the order of 30%, comes from the interatomic $s-p$ interaction, which has not been considered in the literature so far.

In the case of FeTe [H1, H2] and CuMnSb [H3], the coupling between TM ions is of fundamental importance, determining the magnetic phase of the system. It is generally assumed that in metallic systems the long-range RKKY coupling, related to the interaction of d(TM) electrons with band electrons, dominates. As shown, in both crystals the magnetic coupling between TM ions depends on the density of states at the Fermi level (as expected). The low density of states, typical for semimetals, in turn causes a weakening of the long-range RKKY interactions and a dominant role of the short-range interactions (direct exchange and/or superexchange). In FeTe the density of states can be changed by the chemical composition or external pressure, which leads to a change of the antiferromagnetic phase to a ferromagnetic phase or to a change of the magnetic order to a superconducting order. In CuMnSb epitaxial layers, the coexistence of two magnetic phases, antiferromagnetic and ferromagnetic, results from the different densities of states at the Fermi level for the two equilibrium crystallographic structures, cubic and tetragonal. Consequently, the crystallographic polymorphism of CuMnSb layers leads to the magnetic polymorphism.

In most of the works, theoretical and experimental results were compared, and good agreement was achieved both for FeTe [H1, H2] and CuMnSb [H3], as well as for ZnO:Fe, Mn, i Co [H5-H7]. This shows

that the frequently used LDA/GGA approximations with $+U$ corrections are satisfactorily accurate.

References

[1] J. Paglione and R. L. Greene, Nat. Phys. **6**, 645 (2010); G. R. Stewart, Rev. Mod. Phys. **83**, 1589 (2011); Q. Si *et al.*, Nat. Rev. Mater. **1**, 16017 (2016).

[2] M. H. Fang *et al.*, Phys. Rev. B **78**, 224503 (2008); K. W. Yeh *et al.*, Europhys. Lett. **84**, 37002 (2008); Z. Xu *et al.*, Phys. Rev. B **82**, 104525 (2010).

[3] S. Li *et al.*, Phys. Rev. B **79**, 054503 (2009); W. Bao *et al.*, Phys. Rev. Lett. **102**, 247001 (2009); E. E. Rodriguez *et al.*, Phys. Rev. B **84**, 064403 (2011); C. Stock *et al.*, Phys. Rev. B **84**, 045124 (2011).

[4] M. Bendele *et al.*, Phys. Rev. B **87**, 060409(R) (2013).

[5] Y. Mizuguchi *et al.*, Appl. Phys. Lett. **94**, 012503 (2009); R. Hu *et al.*, Phys. Rev. B **80** 214514 (2009); P. Zajdel *et al.*, J. Am. Chem. Soc. **132** 13000 (2010); C. Dong *et al.*, J. Phys.: Condens. Matter **25**, 385701 (2013).

[6] Y. Han *et al.*, Phys. Rev. Lett. **104**, 017003 (2010).

[7] T. Jungwirth *et al.*, Nat. Nanotechnol. **11**, 231 (2016); *idem*, Nat. Phys. **14**, 200 (2018).

[8] M. Law *et al.*, Nat. Mater. **4**, 455 (2005); K. Maeda *et al.*, J. Am. Chem. Soc. **127**, 8286 (2005); S. G. Kumar and K. S. R. K. Rao, RSC Adv. **5**, 3306 (2015); M. Samadi *et al.*, Thin Solid Films **605**, 2 (2016).

[9] T. Dietl, Nat. Mater. **9**, 965 (2010); T. Dietl and H. Ohno, Rev. Mod. Phys. **86**, 187 (2014).

[10] P. Wojnar *et al.*, Nano Lett. **12**, 3404 (2012); J. Kobak *et al.*, Nat. Commun. **5**, 3191 (2014); M. Szymura *et al.*, Nano Lett. **15**, 1972 (2015).

[11] P. Hohenberg and W. Kohn, Phys. Rev. **136**, B864 (1964).

[12] W. Kohn and L. J. Sham, Phys. Rev. **140**, A1133 (1965).

[13] J. F. Janak, Phys. Rev. B **18**, 7165 (1978).

[14] J. P. Perdew *et al.*, Phys. Rev. Lett. **49**, 1691 (1982).

[15] O. A. Vydrov *et al.*,, J. Chem. Phys. **126**, 154109 (2007).

[16] J. P. Perdew and Y. Wang, Phys. Rev. B **45**, 13244 (1992).

[17] J. P. Perdew, K. Burke and M. Ernzerhof, Phys. Rev. Lett. **77**, 3865 (1996).

[18] M. Cococcioni and S. de Gironcoli, Phys. Rev. B **71**, 035105 (2005).

[19] A. Subedi *et al.*, Phys. Rev. B **78**, 134514 (2008); F. Ma *et al.*, Phys. Rev. Lett. **102**, 177003 (2009); M. J. Han and S. Y. Savrasov, Phys. Rev. Lett. **103**, 067001 (2009); C. Y. Moon and H. J. Choi, Phys. Rev. Lett. **104**, 057003 (2010); H. Shi *et al.*, J. Appl. Phys. **110**, 043917 (2011); S. C. Tang *et al.*, Sci. Rep. **6**, 19031 (2016).

[20] A. Ciechan, M. J. Winiarski, M. Samsel-Czekała, Acta Phys. Pol. A **121**, 820 (2012). *idem*, Intermetallics **41**, 44-50 (2013).

[21] M. J. Winiarski, M. Samsel-Czekała, A. Ciechan, *idem*, Europhys. Lett. **100**, 47005, (2012); *idem*, J. Alloys Compd. **566**, 187 (2013); *idem*, Intermetallics **52**, 97 (2014).

[22] M. J. Winiarski, M. Samsel-Czekała, A. Ciechan, *idem*, J. Appl. Phys. **116**, 223903 (2014); *idem*, Mat. Chem. Phys. **186**, 492 (2017).

[23] F. Máca *et al.*, Phys. Rev. B **94**, 094407 (2016).

[24] S. Lany, H. Raebiger and A. Zunger, Phys. Rev. B **77**, 241201(R) (2008).

[25] P. Giannozzi *et al.*, J. Phys. Condens. Matter **21**, 395502 (2009); www.quantum-espresso.org.

[26] Y. Mizuguchi *et al.*, Appl. Phys. Lett. **93**, 152505 (2008); S Medvedev *et al.*, Nature Mater. **8**, 630 (2009); S. Margadonna *et al.*, Phys. Rev. B **80** 064506 (2009); H. Okabe *et al.*, Phys. Rev. B **81**, 205119 (2010).

[27] H. Okada *et al.*, J. Phys. Soc. Japan **78**, 083709 (2009).

[28] Y. Qiu *et al.*, Phys. Rev. Lett. **103**, 067008 (2009); M. S. Lumsden *et al.*, Nat. Phys. **6**, 182 (2010).

[29] A. R. Lennie, *et al.*, Miner. Mag. **59**, 677 (1995).

[30] R. H. Forster *et al.*, J. Phys. Chem. Solids **29**, 855 (1968).

[31] T. Jeong *et al.*, Phys. Rev. B **71**, 184103 (2005).

[32] P. Wadley *et al.*, Sci. Rep. **5**, 17079 (2015); S. Reimers *et al.*, Nat. Commun. **13**, 724 (2022); S. F. Poole *et al.*, Appl. Phys. Lett. **121**, 052402 (2022); A. G. Linn *et al.*, npj Quantum Mater. **8**, 19 (2023); M. J. Grzybowski *et al.*, Phys. Rev. Lett. **118**, 057701 (2017).

[33] F. Máca *et al.*, J. Magn. Magn. Mater. **324**, 1606 (2012); *idem*, Phys. Rev. B **96**, 094406 (2017).

[34] H. Raebiger, S. Lany and A. Zunger, Phys. Rev. B **79**, 165202 (2009); M. A. Gluba and N. H. Nickel, Phys. Rev. B **87**, 085204 (2013).

[35] P. Koidl, Phys. Rev. B **15**, 2493 (1977); H. J. Schulz and M. Thiede Phys. Rev. B **35**, 18 (1987); H. Matsui and H. Tabata, J. Appl. Phys. **113**, 183525 (2013); C. Renero-Lecuna *et al.*, Chem. Mater. **26**, 1100 (2014).

[36] W. Pacuski *et al.*, Phys. Rev. B **73**, 035214 (2006).

[37] S. G. Gilliland *et al.*, Appl. Phys. Lett. **96**, 241902 (2010).

[38] K. R. Kittilstved *et al.*, Nat. Mater. **5**, 291 (2006); C. A. Johnson *et al.*, Phys. Rev. B **81**, 125206 (2010); *idem*, Phys. Rev. B **84**, 125203 (2011).

[39] E. Badaeva *et al.*, J. Phys. Chem. C **113**, 8710 (2009); J. May *et al.*, J. Phys. Chem. C **118**, 13152 (2014); Y. L. Su *et al.*, Solid State Commun. **250**, 123 (2017).

[40] M. Godlewski *et al.*, Opt. Mater. **31**, 1768 (2009); C. A. Johnson *et al.*, Phys. Rev. B **82**, 115202 (2010).

[41] W. Pacuski *et al.*, Phys. Rev. B **84**, 035214 (2011).

[42] K. J. Kim and Y. R. Park, J. Appl. Phys. **96**, 4150 (2004); D. Karmakar *et al.*, Phys. Rev. B **75**, 144404 (2007); Y. Lin *et al.*, J. Alloys Compd. **436**, 30 (2007).

[43] R. Heitz, A. Hoffmann and I. Broser, Phys. Rev. B **45**, 8977 (1992).

[44] A. Janotti and C. G. Van de Walle, Phys. Rev. B **76**, 165202 (2007); F. Oba *et al.*, Phys. Rev. B **77**, 245202 (2008).

[45] K. Ando, J. Appl. Phys. **89**, 7284 (2001).

[46] W. Przeździecka *et al.*, Solid State Commun. **139**, 541 (2006); *idem*, Phys. Stat. Sol. c **3**, 988 (2006).

[47] T. Mizokawa *et al.*, Phys. Rev. B **65**, 085209 (2002); D. A. Schwartz *et al.*, J. Am. Chem. Soc. **125**, 13205 (2003); J. Okabayashi *et al.*, J. Appl. Phys. **95**, 3573 (2004).

[48] B. E. Larson, Phys. Rev. B **37**, 4137 (1988); A. K. Bhattacharjee, Phys. Rev. B **46**, 5266 (1992); J. Blinowski and P. Kacman, Phys. Rev. B **46**, 12298 (1992); P. Kacman, Semicond. Sci. Technol. **16**, R25 (2001); S. Sanvito, P. Ordejón and N. A. Hill, Phys. Rev. B **63**, 165206 (2001); L. M. Sandratskii, Phys. Rev. B **68**, 224432 (2003).

[49] T. Chanier, F. Virot and R. Hayn, Phys. Rev. B **79**, 205204 (2009); R. Beaulac and D. R. Gamelin, Phys. Rev. B **82**, 224401 (2010).

[50] K. Sato *et al.*, Rev. Mod. Phys. **82**, 1633 (2010).

[51] S. H. Liu, Phys. Rev. **121**, 451 (1961).

5 Presentation of significant scientific activity

Maria Curie-Sklodowska University, Lublin

- 2003 - 2004 - the last year of master's studies under supervision of prof. dr hab. K. I. Wysokiński resulted in the first, co-authored scientific publication on *"Relativistic effects in superconductors"* ([M1] from the list of scientific publications in the section 7.2) and presentation of the results at the conference ([R1] from section 7.4).
- 2004 - 2010 (with a break for maternity leave) - doctoral studies in physics under supervision of prof. dr hab. K. I. Wysokiński, during which I conducted theoretical research on
  - superconductivity in metallic grains described by the two-level Richardson model;
  - superconductivity in multiband systems;
  - interorbital effects in two-band inhomogeneous superconductors;
  - description of superconductivity in iron pnictides;

  as well as
  - I participated in 2 research projects [G1, G2] as an investigator, including a supervisory grant [G2] (list of grants is presented in section 7.3);
  - I was a co-author of 9 scientific publications [M1-M9], another one [D1] was also the result of research conducted during PhD studies;
  - I participated in scientific conferences [R1-R10] and gave on average 2 presentations per year between 2004 and 2010 at physics seminars for PhD students.

Institute of Physics of Polish Academy of Sciences, Warsaw

- since 2010 - assistant professor and then assistant in Division of Physics of Magnetism (ON3) in the group prof. dr hab. R. Puźniak. During my employment I conducted theoretical calculations using density functional theory. The subject of my interests was
  - Fe(Se,Te) iron superconductors: Fe(Se,Te) research contributed to the settlement of grants [G3], [G5-G7] and resulted in publications [D2-D8], [H1, H2];
  - doped ZnO semiconductor: participation in a grant as an investigator [G6] and in own grant [GW] and publications being the basis for the scientific achievement [H4-H8];
  - magnetically doped topological insulators Bi_2Se_3: grant [GW], publication [D9];
  - defects and magnetic properties of semi-Heusler CuMnSb alloys: publication [H3];
  - olivines $LiTMPO_4$, TM = Mn, Fe, Ni, Co (ad hoc): grant [G4].

The results of my research at IP PAS were presented many times at national and international conferences, seminars and other presentations.

Scientific cooperation

- cooperation at the Institute of Physics of PAS
  - 2011-2012 – cooperation with the group carrying out the project [G4], the task concerning the use of olivines $LiTMPO_4$, TM = Mn, Fe, Ni and Co, in lithium batteries (including prof. dr hab. A. Szewczyk, prof. dr hab. A. Wiśniewski, dr M. Gutowska, dr J. Więckowski from my division **ON3** and co-executors of the task from **AGH University of Science and Technology** in Cracow, including prof. dr hab. inż. J. Molenda);
  - since 2013 – close cooperation with prof. dr hab. Piotr Bogusławski (Division **ON5**) regarding DFT calculations for ZnO and CuMnSb;

- 2015-2016 – cooperation with prof. dr hab. A. Suchocki, dr hab. H. Przybylińska and dr A. Grochot (Division **ON4**) and with prof. dr hab. A. Mycielski, dr hab. A. Grasza and dr P. Skupiński (Division **ON1**) concerning the interpretation of photo-EPR spectra for the Mn-doped ZnO;
- 2022-2024 – cooperation with groups from Laboratory **SL2** (prof. dr hab. M. Sawicki, dr K. Gas) and **SL1** (dr hab. P. Dłużewski, dr hab. S. Kret), as well as international cooperation with group from **Faculty of Physics and Astronomy, Julius Maximilian University of Würzburg** (dr L. Scheffler, prof. C. Gould, dr J. Kleinlein and prof. L. W. Molenkamp) concerning the structural and magnetic properties of CuMnSb.

- cooperation beyond the Institute of Physics of PAS
  - 2011-2016 – cooperation with **Institute of Low Temperature and Structure Research of the Polish Academy of Sciences** in Wroclaw (dr hab. M. Samsel-Czekała, dr hab. M. J. Winiarski) - calculations of the electronic band structure of iron superconductors Fe(Se,Te);
  - 2015-2016 – cooperation with **Institute of Experimental Physics of the University of Warsaw** (prof. dr hab. M. Nawrocki, prof. dr hab. A. Twardowski, dr hab. A. Drabińska, dr hab. G. Kowalski, dr hab. J. Szczytko, dr hab. W. Pacuski, dr hab. J. Suffczyński, dr M. Tokarczyk, mgr A. Gardias, mgr J. Papierska, mgr K. Sawicki) and with **National Science Centre in Giza** in Egypt (prof. M. Boshta, prof. M. M. Gomaa) and with **University of Versailles St-Quentin en Yvelines-CNRS** in France (dr E. Chikoidze and prof. Y. Dumont) - DFT calculations vs. experimental data for ZnO doped by Fe;
  - 2019-2021 – cooperation with dr hab. K. Kapcia (currently **Faculty of Physics, Adam Mickiewicz University** in Poznan) and dr hab. A. Ptok (**Institute of Nuclear Physics, Polish Academy of Sciences** in Cracow) - calculations of the electronic structure of topological insulators $(Bi,Sb)_2(Se,Te)_3$ doped with magnetic ions Mn, Fe, Co, Ni.

6 Presentation of teaching and organizational achievements as well as achievements in popularization of science

6.1 Teaching

- Maria Curie-Sklodowska University, Lublin
  - exercises for the lecture *„Physics”*,
    master's studies at the Faculty of Chemistry, UMCS,
    4 semesters of 30-60 hours in the academic years 2004/2005 and 2005/2006
  - exercises in the subject *"Selected issues of modern physics"*,
    master's studies at the Institute of Physics UMCS,
    30 hours in the winter semester 2007/2008

- Institute of Physics of Polish Academy of Sciences, Warsaw:
  - exercises for the lecture *"Solid State Physics - Magnetism and Superconductivity"*,
    PhD studies at Institute of Physics PAS,
    8 hours in the summer semester 2014/2015
  - lecture *"Solid State Physics - Magnetism and Superconductivity"*,
    PhD studies at Institute of Physics PAS,
    16 hours in the summer semester 2016/2017

6.2 Organization of conferences

- XI National School of Superconductivity, "Collective Phenomena and Their Competition",
  Kazimierz Dolny, 25-29.09.2005,
  member of the local organizing committee

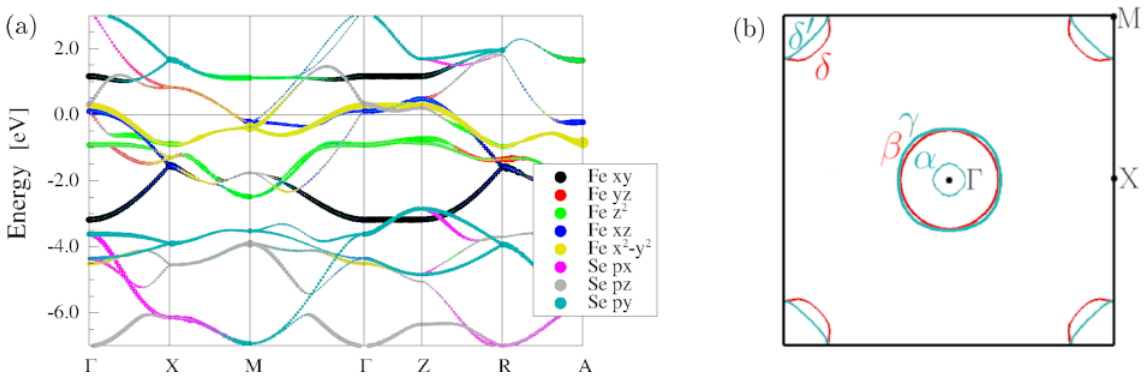

Figure 15: (a) FeSe band structure with visible contributions from d(Fe) and p(Se) orbitals and (b) the Fermi surface in the $k_z = 0$ plane. Hole sheets are located around the Γ point, and electron ones around the M point.

7 Other information about professional career

7.1 Additional scientific achievement: „Research on the band structure of superconducting iron chalcogenides" [D2-D8]

The description of multiband superconductors, and in particular the role of nonmagnetic impurities in multiband superconductors, was the subject of my PhD dissertation ([M6-M8] from section 7.2). These were model studies based on the Bogoliubov-de Gennes equations, in which the influence of impurities on the parameters of the superconducting state, i.e. order parameters and critical temperature, was considered. It was shown that in iron-based superconductors, the interorbital interaction of d(Fe) electrons can lead to the appearance of a superconducting gap in the density of states below the critical temperature. After starting work at IP PAS and mastering basic DFT techniques, I started studying Fe(Se,Te) superconductors in the normal state (i.e. non-superconducting state). At that time, Fe(Se,Te) compounds were intensively studied experimentally in my research division, the Division of Physics of Magnetism, IP PAS, under management of prof. dr hab. R. Puźniak, as well as at the Institute of Low Temperatures and Structural Research of Polish Academy of Sciences, INTiBS PAS, in Wroclaw. The series of papers [D2-D8], presented in section 7.2, concerns the studies of the electronic band structure of iron chalcogenides, which I conducted in collaboration with dr. hab. M. Winiarski and dr. hab. M. Samsel-Czekała from INTiBS PAN.

In the papers [D2-D7], LDA/GGA calculations of the band structure of iron chalcogenides are nonmagnetic calculations, i.e. they were performed without spin polarization. They show a metallic band structure with bands originating mainly from d(Fe) electrons around the Fermi level [D2]. They form a Fermi surface with cylindrical hole and electron sheets, presented in Figure 15. Fluctuations related to the so-called *nesting* of the Fermi surface sheets, i.e. overlapping of electron and hole sheets (β and δ sheets from Figure 15 (b)) after shifting by the vector $\mathbf{q}_{nest} = (\pi, \pi)$, are believed to play an important role in interband electron pairing in the superconducting state. Indeed, the enhancement of such fluctuations seen in neutron scattering spectra [1] correlates with the increase of the critical temperature of Fe(Se,Te) compounds. Our theoretical works also indicate correlations between the band structure obtained by DFT methods and the experimentally observed critical temperature of iron superconductors.

In the paper [D4], the effect of the influence of substitution with S and Te ions and the influence of doping with Co, Ni and Cu on the band structure of FeSe was investigated. The critical temperature of the transition to the superconducting state for pure FeSe is $T_c \approx 8$ K. Partial substitution of Se atoms with sulfur weakly affects the critical temperature of $FeSe_{1-x}S_x$ in the range of $x \in (0, 0.2)$. At higher S concentrations the critical temperature decreases and the superconducting state is no longer observed for $x = 0.4$ [2]. Substitutions of Te atoms in Se positions increase the critical temperature of FeSe, which reaches a maximum value of 15 K for $FeSe_{0.5}Te_{0.5}$ [2]. In turn, doping with Ni, Co and Cu ions destroys the superconducting state of FeSe chalcogenides at concentrations of $x < 10\%$ [3]. The $FeSe_{0.875}S_{0.125}$ band structure calculated in [D4] is almost identical to that obtained for pure FeSe. In particular, a decrease in the density of states at the Fermi level is observed, i.e. the so-called pseudogap characteristic of semimetals. The overlap of the hole and electron Fermi surface sheets after shifting by the vector

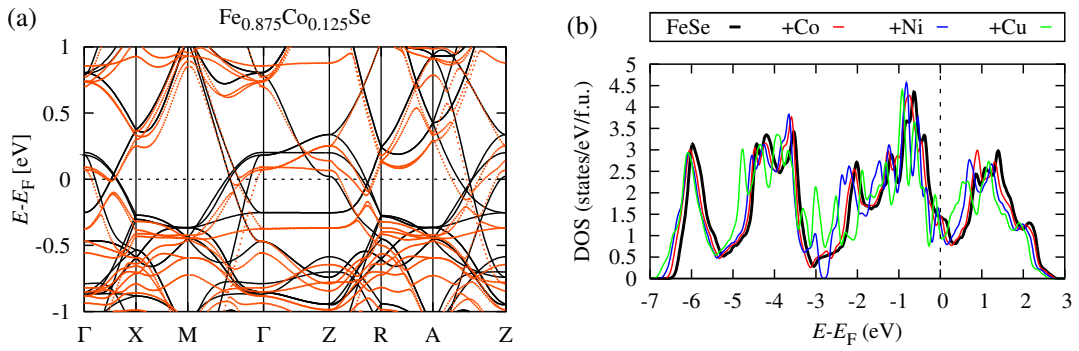

Figure 16: (a) The band structure of FeSe:Co in orange against the background of pure FeSe structure shown in black. (b) Shifting of the FeSe density of states towards lower energies due to doping of Co, Ni and Cu.

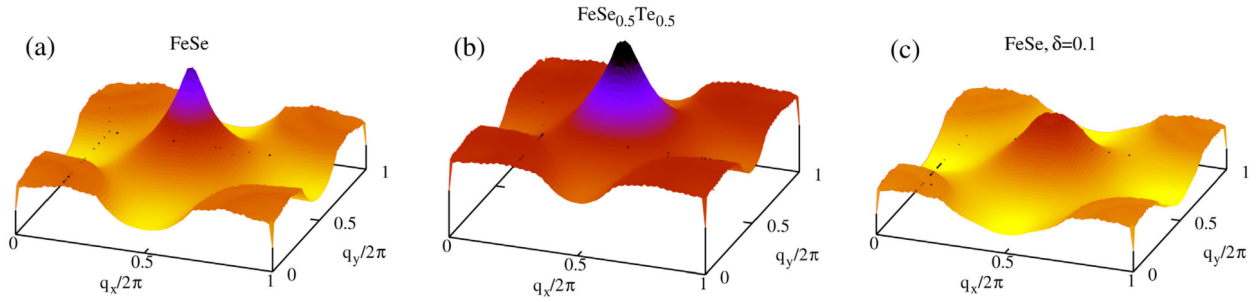

Figure 17: The noninteracting spin susceptibilities $\chi(\omega \to 0)$ of (a) pure FeSe, (b) $FeSe_{0.5}Te_{0.5}$,s and (c) FeSe with additional 0.1 electron per formula unit.

$\mathbf{q}_{nest} = (\pi, \pi)$ occurs mainly in the $q_z = 0$ plane. In $FeSe_{0.5}Te_{0.5}$, on the other hand, there are clear changes in the electronic structure. The density of states at the Fermi level increases slightly, giving rise to larger Fermi surface sheets and providing optimal conditions for enhanced spin fluctuations.

The largest changes in the band structure were observed for FeSe doped with transition metal ions Co, Ni and Cu. It was shown that the hole sheets shrink and the electron sheets enlarge, and these changes occur most rapidly in the case of Cu. The main modification of the FeSe:Co band structure, even at a relatively high dopant concentration of 12.5%, shown in Figure 16 (a), is the shift of all bands towards lower energies compared to the parent compound. Such a situation corresponds to the increase in electron concentration in the cell, which leads to the upshift of the Fermi level. A similar effect is also seen for Ni and Cu in Figure 16 (b). The dopant concentrations that destroy the superconducting state of FeSe are 10% Co, 5% Ni and 3% Cu [3]. All these concentrations correspond to doping by 0.1 electrons per formula unit and shift the Fermi level by about 0.07 eV. This observation allowed us to describe the electronic structure changes for these critical concentrations using the rigid bands model.

The spin fluctuations due to nesting were estimated by calculating the spin susceptibility in a standard 4-atom FeSe cell:

$$\chi(\mathbf{q}, \omega) = -\frac{1}{(2\pi)^3} \sum_{\mathbf{k} \in BZ} \sum_{m,n} \frac{f(\varepsilon_{m,\mathbf{k}}) - f(\varepsilon_{n,\mathbf{k}+\mathbf{q}})}{\varepsilon_{m,\mathbf{k}} - \varepsilon_{n,\mathbf{k}+\mathbf{q}} - \omega}. \tag{10}$$

In the above equation, $\varepsilon_{m,\mathbf{k}}$ and $\varepsilon_{n,\mathbf{k}+\mathbf{q}}$ denote the energy of the hole and electron bands for the wave vector $\mathbf{k}$ and $\mathbf{k}+\mathbf{q}$, and $f(\varepsilon_{m,\mathbf{k}})$ and $f(\varepsilon_{n,\mathbf{k}+\mathbf{q}})$ are the Fermi-Dirac distribution functions. Figure 17 shows the static susceptibility $\chi(\omega \to 0)$ in the $q_z = 0$ plane for FeSe, $FeSe_{0.5}Te_{0.5}$ and electron-doped FeSe. The peak at $\mathbf{q}_{nest} = (\pi, \pi)$ indicates the presence of spin fluctuations in FeSe and $FeSe_{0.5}Te_{0.5}$. The spin susceptibility calculated for $FeSe_{0.5}Te_{0.5}$ is characterized by a higher and more extended peak at $\mathbf{q}_{nest}$, indicating stronger antiferromagnetic fluctuations in this chalcogenide. This is correlated with the higher transition temperature of $FeSe_{0.5}Te_{0.5}$ to the superconducting state. For electron-doped FeSe, the peak at $\mathbf{q}_{nest} = (\pi, \pi)$ is strongly weakened indicating the disappearance of spin fluctuations. This is correlated with the disappearance of the superconducting state.

The work [D2] concerns the effect of hydrostatic pressure on the band structure of FeSe and $FeSe_{0.5}Te_{0.5}$. It was shown that the density of states at the Fermi level increases under pressure, and the β and δ sheets become more corrugated. This leads to stronger fluctuations in the vicinity of the (π, π) point, while an increase in the critical temperature is observed in the experiment [4]. Similar effects related to the Fe(Se,Te) band structure were also studied for axial pressures, i.e. compressive and tensile stresses of the layers in the *ab* plane (which can occur in epitaxial layers) or along the *c* axis (e.g. under the influence of substitutions, i.e. chemical pressure) [D3, D5, D6]. The results clearly indicate that in the superconducting state the spin fluctuations visible in the susceptibility $\chi(\mathbf{q})$ as a broad peak around the vector $\mathbf{q}_{nest} = (\pi, \pi)$ are important and that they are directly related to the band structure of these compounds.

Referring to the scientific achievements of [H1] and [H2], a strong connection between spin fluctuations and superconductivity is seen in DFT studies of the nonmagnetic band structure as well as in studies of the magnetic ground state of iron chalcogenides. Both of these approaches were used in [D6]. In FeTe under *ab*-plane tensile strain, the calculated magnetic ground state is an order in the form of single stripes in the direction [110], see Figure 3, i.e. the order associated with the propagation vector $\mathbf{q}_{nest} = (\pi, \pi)$. We can therefore rightly conclude about the presence of a superconducting state. At the same time, it was shown that similar conclusions can be reached by taking into account the topology of the Fermi surface and the susceptibility $\chi(\mathbf{q})$ obtained from calculations without spin polarization.

The presence of partially nested Fermi surface sheets causes strong instability of the system. One can expect that perfect nesting (sharp, narrow peak in $\chi(\mathbf{q}_{nest})$) lead to the occurrence of an antiferromagnetic state or a spin density wave state, SWD, in the system. Imperfect nesting, due to the 3-dimensionality of the Fermi sheets, differences in the shape and/or size of the cylinders, causes the broadening of the peak at (π, π) and competition between SWD and superconductivity. However, in DFT calculations where the superconducting state is not considered, the magnetically stable state is the antiferromagnetism associated with (π, π) fluctuations. In the case of weak nesting, i.e. weak overlap of the sheets after shifting by $\mathbf{q}_{nest} = (\pi, \pi)$, the spin fluctuations weaken and both the SWD and the superconducting state disappear.

Finally, similar band structure and magnetic properties have also been observed in hypothetical ruthenium compounds, $Ru_xFe_{1-x}Se$ and $Ru_xFe_{1-x}Se$ [D7, D8], making them potential candidates for superconductors.

The articles [D2-D8] were used to settle the European grant "FunDMS", managed by prof. dr hab. T. Dietl (grant [G3] from the list in section 7.3), and three NCN projects managed by prof. dr hab. R. Puźniak [G5, G7] and prof. dr hab. P. Bogusławski [G6]. The results of the works were presented at national and international conferences (from the list in section 7.4: invited lecture [Z1], poster presentations [P1, P7, P9, P10, P12]), seminars and other oral presentations [S2, S4, S6-S9].

Individual contribution:

- In paper [D2] I performed DFT calculations of changes in the crystallographic structure of FeSe and $FeSe_{0.5}Te_{0.5}$ under pressure, and dr hab. M. Winiarski calculated the band structure of these compounds.
- In paper [D4] I performed all the calculations and was the main author of the publication text.
- In articles [D3, D5, D6] the calculations were performed by dr hab. M. Winiarski. I participated in the interpretation of the results and editing of the text of the publication. The research on the spin susceptibility of Fe(Se,Te) superconductors was a continuation of the research presented in [D4].
- The calculations presented in [D6-D8] were obtained by dr hab. M. Winiarski. I took part in the interpretation of the obtained results and the final editing of the text. The works were a continuation of the magnetic calculations proposed in the habilitation achievement [H1].

References

[1] Y. Qiu *et al.*, Phys. Rev. Lett. **103**, 067008 (2009); M. S. Lumsden *et al.*, Nat. Phys. **6**, 182 (2010).

[2] Y. Mizuguchi and Y. Takano, J. Phys. Soc. Jpn. **79**, 102001 (2010).

[3] A. J. Williams *et al.*, J. Phys. Condens. Matter **21**, 305701 (2009); Y. Mizuguchi *et al.*, J. Phys. Soc. Jpn. **78**, 074712 (2009); M. K. Wu *et al.*, Physica C **469**, 340 (2009); B. L. Young *et al.*, Phys. Rev. B **81**, 144513 (2010).

[4] Y. Mizuguchi *et al.*, *Appl. Phys. Lett.* **93**, 152505 (2008); S. Margadonna *et al.*, *Phys. Rev. B* **80**, 064506 (2009); K. Horigane *et al.*, *J. Phys. Soc. Jpn.* **78**, 063705 (2009); N. C. Gresty *et al.*, *J. Am. Chem. Soc.* **131**, 16944 (2009).

7.2 Publications not included in the scientific achievement

Publications before PhD

[M1] A. Ciechan, A. Donabidowicz and K. I. Wysokiński, *„Relativistic Theory of Superconductivity: BCS vs. Bogoliubov – de Gennes Approaches"*, Acta Physica Polonica A **106**, 699 (2004).

[M2] A. Ciechan and K. I. Wysokiński, *„Finite Size Corrections in the Two-Level BCS Model"*, Acta Physica Polonica A **109**, 569 (2006).

[M3] A. Ciechan and K. I. Wysokiński, *„Thermodynamics of the Two-Level Richardson Model"*, Acta Physica Polonica A **111**, 467 (2007).

[M4] A. Ciechan and K. I. Wysokiński, *„Pairing Correlations around Negative-U Centre in the Two-Band Model"*, Acta Physica Polonica A **114**, 123 (2008).

[M5] A. Ciechan, J. Krzyszczak and K. I. Wysokiński, *„Theoretical analysis of STM spectra in cuprate and pnictide superconductors"*, Acta Physicae Superficierum **XI**, 18 (2009).

[M6] A. Ciechan, J. Krzyszczak, K. I. Wysokiński, *„Inhomogeneities in superconductors: two component and two band scenarios"*, Journal of Physics: Conference Series **150**, 052283 (2009).

[M7] A. Ciechan and K. I. Wysokiński, *„Interorbital pair scattering in two-band superconductors"*, Physical Review B **80**, 224523 (2009).

[M8] A. Ciechan and K. I. Wysokiński, *„Inter-orbital Effects in the Impure Pnictide Superconductors"*, Acta Physica Polonica A **118**, 356 (2010).

[M9] K. I. Wysokiński, A. Ciechan and J. Krzyszczak, *„Theoretical analysis of short coherence length superconductors"*, Acta Physica Polonica A **118**, 232 (2010).

Publications after PhD

[D1] A. Ciechan and K. I. Wysokiński, *„Interorbital pairs in clean and impure superconductors"*, Journal of Physics: Conference Series **303**, 012111 (2011).

[D2] A. Ciechan, M. J. Winiarski, M. Samsel-Czekała, *„The Pressure Effects on Electronic Structure of Iron Chalcogenide Superconductors $FeSe_{1-x}Te_x$"*, Acta Physica Polonica A **121**, 820 (2012).

[D3] M. J. Winiarski, M. Samsel-Czekała, A. Ciechan, *„Strain effects on the electronic structure of the iron selenide superconductor"*, Europhysics Letters **100**, 47005 (2012).

[D4] A. Ciechan, M. J. Winiarski and M. Samsel-Czekała, *„The substitution effects on electronic structure of iron selenide superconductors"*, Intermetallics **41**, 44-50 (2013).

[D5] M. J. Winiarski, M. Samsel-Czekała, A. Ciechan, *„Strain effects on the electronic structure of the $FeSe_{0.5}Te_{0.5}$ superconductor"*, Journal of Alloys and Compounds **566**, 187 (2013).

[D6] M. J. Winiarski, M. Samsel-Czekała, A. Ciechan, *„Strain effects on electronic structure and superconductivity in the iron telluride"*, Intermetallics **52**, 97 (2014).

[D7] M. J. Winiarski, M. Samsel-Czekała, A. Ciechan, *„Electronic structure of ruthenium-doped iron chalcogenides"*, Journal of Applied Physics **116**, 223903 (2014).

[D8] M. J. Winiarski, M. Samsel-Czekała, A. Ciechan, *„Strain effects on electronic structure of* $Fe_{0.75}Ru_{0.25}Te$*"*, Materials Chemistry and Physics **186**, 492 (2017).

[D9] A. Ptok, K. J. Kapcia, A. Ciechan, *„Electronic properties of* Bi_2Se_3 *dopped by 3d transition metal (Mn, Fe, Co, or Ni) ions"*, Journal of Physics: Condensed Matter **33**, 065501 (2021).

7.3 Research grants

Management of the own grant:

[GW] grant NCN UMO-2016/21/D/ST3/03385 *„Properties of Transition Metal Ions in Wide-Gap Semiconductors and Three-Dimensional Topological Insulators"* (IP PAS, 2017-2021).

Participation in research projects as a contractor:

[G1] grant KBN Nr N N 202 187833 *„Quantum Transport and Superconductivity in Solid and Nanoscopic Materials"* managed by prof. dr hab. K. I. Wysokiński (UMCS, 2007-2009);

[G2] dissertation grant KBN Nr N N202 169836 *„Properties of multiband superconductors* $LaFeAsO_{1-x}F_x$ *– thermodynamics and STM spectra"* managed by prof. dr hab. K. I. Wysokiński (UMCS, 2009-2010);

[G3] Advanced Grant of the European Research Council, FP7 "Ideas", nr 227690 *„FunDMS - Functionalization of Diluted Magnetic Semiconductors"* managed by prof. dr hab. T. Dietl (IP PAS, 2011-2013);

[G4] European grant in the Innovative Economy program, Nr POIG 01.01.02-00-108/09 *„Modern Materials and Innovative Methods for Energy Processing and Monitoring (MIME)"* managed by prof. dr hab. A. Suchocki (IP PAS, 2011-2013);

[G5] grant NCN No. DEC-2011/01/B/ST3/02374 *„The influence of chemical substitutions, hydrostatic pressure and defects on the properties of the superconducting state of iron-based compounds"* managed by prof. dr hab. R. Puźniak (IP PAS, 2011-2014);

[G6] grant NCN No. DEC-2012/05/B/ST3/03095 *„Electron-electron interaction in crystals containing transition metal ions: dependence of the exchange-correlation correction '+U' on the ion environment"* managed by prof. dr hab. P. Bogusławski (IP PAS, 2013-2015);

[G7] grant NCN No. DEC-2013/08/M/ST3/00927 *„Modification of the Superconducting State Properties of Layered Superconductors by Chemical Substitution and Intercalation"* managed by prof. dr hab. R. Puźniak (IP PAS, 2013-2016).

7.4 Conferences, seminars and other presentations

Conference presentations

Invited speech:

[Z1] M. Samsel-Czekała, M. J. Winiarski, A. Ciechan, *„Magnetism and superconductivity in strained and doped iron chalcogenides"*, co-author of an invited lecture at the conference 'From Spins to Cooper Pairs: New Physics of the Spins (StoCP- 2014)', 22-26.09.2014, Zakopane, Poland.

[Z2] A. Ciechan, P. Bogusławski, *„Transition metal ions in ZnO: effects of intra-shell Coulomb repulsion on electronic properties"*, presentation of results at 'Phosphor Safari and The Sixth International Workshop on Advanced Spectroscopy and Optical Materials (PS- IWASOM'17)', 9-14.07.2017, Gdansk, Poland.

Oral presentations:

[O1] A. Ciechan, M. J. Winiarski and M. Samsel-Czekała, *„The pressure effect on magnetism and superconductivity of FeTe"*, presentation of results at the conference 'E-MRS 2014 Fall Meeting', Symposium O: 'Recent progress in new high-Tc superconductors and related multifunctional and magnetic materials', 15-19.09.2014, Warsaw, Poland.

[O2] A. Ciechan, *„Magnetism of strained and S-substituted FeTe: DFT study"*, oral presentation at 'XVII National Superconductivity Conference: Superconductivity and other emergent states in systems with strongly correlated electrons', 25-30.10.2015, Karpacz, Poland.

[O3] A. Ciechan, *„Magnetic Phase Transitions in Iron Chalcogenides: DFT Calculations"*, oral presentation at 'Symposium on Computational Ab Initio Methods', 29.02.2016, Institute of Nuclear Physics of Polish Academy of Sciences, Cracow, Poland.

[O4] J. Papierska, A. Ciechan, P. Bogusławski, M. Boshta, M. M. Gomaa, E. Chikoidze, Y. Dumont, A. Drabińska, H. Przybylińska, A. Gardias, J. Szczytko, A. Twardowski, M. Tokarczyk, G. Kowalski, B. Witkowski, K. Sawicki, W. Pacuski, M. Nawrocki, and J. Suffczyński, *„Physics of iron dopant in ZnO: 3+ valency and s, p-d exchange interaction"*, co-author of presentation at '33rd International Conference on the Physics of Semiconductors', 31.07-05.08.2016, Beijing, China.

[O5] A. Ciechan, P. Bogusławski, *„Transition metal dopants in ZnO: magnetic and optical properties"*, presentation at 'II Symposium on Computational Ab Initio Methods', 12-13.03.2018, Institute of Nuclear Physics of Polish Academy of Sciences, Cracow, Poland.

[O6] P. Bogusławski, A. Ciechan, *„Transition metal ions in ZnO: theory of the $s, p-d$ exchange coupling"* co-author of presentation at The European Conference 'Physic of Magnetism 2021', 28.06-02.07.2021, Poznan, Poland.

Poster presentations:

[P1] A. Ciechan, M. J. Winiarski i M. Samsel-Czekała, *„The effect of pressure on changes in the electronic structure of iron superconductors $FeSe_{1-x}Te_x$"*, presentation at 'XV School of Superconductivity: 100 years of superconductivity', 09-13.10.2011, Kazimierz Dolny, Poland.

[P2] A. Ciechan, S. Markovskyi, M. Gutowski, P. Sybilski, *„Electronic structure of doped $LiFePO_4$ olivines"*, presentation at 'Joint European Magnetic Symposia (JEMS)', 09-14.09.2012, Parma, Italy.

[P3] A. Ciechan, M. J. Winiarski and M. Samsel-Czekała, *„Magnetic phase transitions of FeTe under hydrostatic and biaxial pressure"*, presentation at 'XVI National Superconductivity Conference: Unconventional Superconductivity and Strongly Correlated Systems", 07-12.10.2013, Zakopane, Poland.

[P4] A. Ciechan, M. J. Winiarski and M. Samsel-Czekała, *„Magnetism and superconductivity of strained FeTe"*, presentation at '50th Karpacz Winter School of Theoretical Physics. Quantum Criticality in Condensed Matter: Phenomena, Materials and Ideas in Theory and Experiment', 02-09.03.2014, Karpacz, Poland.

[P5] A. Ciechan, P. Boguslawski, *„The Role of Electronic Correlations in Iron Chalcogenide Superconductors within GGA+U Approach"*, presentation at the workshop 'What about U? – Strong correlations from first principles', 17-20.06.2014, CECAM-HQ-EPFL, Lausanne, Switzerland.

[P6] A. Ciechan, M. J. Winiarski and M. Samsel-Czekała, *„Magnetism and superconductivity of S-substituted FeTe"*, presentation at the European Conference 'Physics of Magnetism 2014', 23-27.06.2014, Poznan.

[P7] A. Wiśniewski, A. Ciechan, R. Puźniak, M. J. Winiarski, M. Samsel-Czekała, D. J. Gawryluk, M. Berkowski, *„Effect of substitutions on superconducting properties of chalcogenides: magnetic studies and band structure calculations"*, co-author of presentation at '27th International Conference on Low Temperature Physics', 6-13.08.2014, Buenos Aires, Argentina.

[P8] A. Ciechan, H. Przybylińska, P. Skupiński, A. Mycielski, P. Bogusławski, A. Suchocki, *„Metastability of Mn^{3+}/Mn^{2+} in ZnO: theory and experiment"*, co-author of presentation at '44th International School & Conference on the Physics of Semiconductors: Jaszowiec 2015', 20-25.06.2015, Wisla, Poland.

[P9] A. Ciechan, M. J. Winiarski, M. Samsel-Czekała, *„Density functional study of TM-doped FeSe: influence of magnetism on superconductivity"*, presentation at 'The 11th International Conference on Materials & Mechanisms of Superconductivity (M2S)', 23-28.08.2015, CICG, Geneva, Switzerland.

[P10] M. Winiarski, , M. Samsel-Czekała, A. Ciechan, *„Strain effects on electronic structure of $Fe_{0.75}Ru_{0.25}Te$"*, co-author of presentation at 'XII National Superconductivity Conference: Superconductivity and other emergent states in systems with strongly correlated electrons', 25-30.10.2015, Karpacz, Poland.

[P11] A. Ciechan, J. Papierska, P. Bogusławski, M. Boshta, M. M. Goma, E. Chikoidze, Y. Dumont, A. Drabinska, H. Przybylińska, A. Gardias, J. Szczytko, A. Twardowski, M. Tokarczyk, G. Kowalski, B. Witkowski, K. Sawicki, W. Pacuski, M. Nawrocki, J. Suffczyński, *„Fe donor in ZnO: a Half-resonant Character Driven by Strong Intracenter Coulomb Coupling"*, co-author of presentation at '45th International School & Conference on the Physics of Semiconductors: Jaszowiec 2016', 18-24.06.2016, Szczyrk, Poland.

[P12] M. Samsel-Czekała , M. Winiarski, A. Ciechan, *„Strain effects on electronic structure of $Fe_{0.75}Ru_{0.25}Te$"*, co-author of presentation at 'Symposium on Computational Ab Initio Methods', 29.02.2016, Institute of Nuclear Physics of Polish Academy of Sciences, Cracow, Poland.

[P13] A. Ciechan, P. Bogusławski, *„Electronic and magnetic structure of 3d impurities in ZnO: Fermi level effects on $p-d$ coupling"*, co-author of presentation at '46th International School & Conference on the Physics of Semiconductors: Jaszowiec 2017', 17-23.06.2017 Szczyrk, Poland.

[P14] A. Ciechan, P. Bogusławski, *„Co dopant in ZnO: ionization vs internal optical transitions"*, presentation at '47th International School & Conference on the Physics of Semiconductors: Jaszowiec 2018', 16-22.06.2018 Szczyrk, Poland.

[P15] A. Ciechan, P. Bogusławski, *„Optical properties of Co-doped ZnO: GGA+U calculations"*, presentation at '10th International Workshop on Zinc Oxide and Other Oxide Semiconductors (IWZnO-2018)', 11-14.08.2018, Warsaw, Poland.

[P16] A. Ciechan, P. Bogusławski, *„Transition metal ions in ZnO: DFT calculations of electronic and magnetic properties"*, presentation at 'Autumn School on Correlated Electrons: Many-Body Methods for Real Materials', 16-20.08.2019, Forschungszentrum Jülich, Niemcy.

[P17] A. Ciechan, P. Bogusławski, *„s, p - d coupling in ZnO doped with 3d transition metal impurities"*, presentation at '49th International School & Conference on the Physics of Semiconductors: Jaszowiec 2021', 01-10.08.2021, Warsaw, Poland/online only.

(before PhD)

[R1] A. Ciechan, A. Donabidowicz, K. I. Wysokiński, *„Relativistic theory of superconductivity BCS vs Bogolubov – de Gennes approaches"*, presentation at 'X National School of Superconductivity: High-temperature superconductivity and other phenomena in perovskites', 06-10.06.2004, Warsaw, Poland.
Honorable Mention for the Best Poster.

[R2] A. Ciechan, K. I. Wysokiński, *„Finite Size Corrections in the Two-Level BCS Model"*, presentation at The European Conference 'Physics of Magnetism '05', 24-27.06.2005, Poznan, Poland.

[R3] A. Ciechan, K. I. Wysokiński, *„Finite Properties of Materials at Nanoscale"*, presentation at 'Conference on Strongly Interacting Systems at the Nanoscale', 08-12.08.2005, Trieste, Italy.

[R4] A. Ciechan, K. I. Wysokiński, *„Superconductivity in small metallic grains"*, presentation at 'XI National School of Superconductivity Collective phenomena and their competition', 25-29.09.2005, Kazimierz Dolny, Poland.

[R5] A. Ciechan, K. I. Wysokiński, *„Superconducting correlations around negative-U centre in metal described by two-band model"*, presentation at 'XIII National School of Superconductivity: Superconductivity, spin and charge ordering', 6-10.11.2007, Ladek Zdroj, Poland.

[R6] A. Ciechan, K. I. Wysokiński, *„Inhomogeneities in two band superconductor: real space approach"*, presentation at the conference 'Competing Orders, Pairing Fluctuations, and Spin Orbit Effects in Novel Unconventional Superconductors', 30.06-4.07.2008, Dresden, Germany.

[R7] A. Ciechan, J. Krzyszczak, K. I. Wysokiński, *„Inhomogeneities in superconductors: two component and two band scenarios"*, co-author of presentation at '25th International Conference on Low Temperature Physics', 2008, Amsterdam, Netherlands.

[R8] A. Ciechan, K. I. Wysokiński, *„Efekty pasmowe w nadprzewodnikach niejednorodnych"*, presentation at 'XIV National School of Superconductivity: Superconductivity and inhomogeneous condensed systems', 13-17.10.2009, Ostrow Wielkopolski, Poland.

[R9] A. Ciechan, K. I. Wysokiński, *„Inter-orbital Effects in the Impure Pnictide Superconductors"*, presentation at 'European Workshop: Electronic Structure of Fe-Based Superconductors', 10-12.05.2010, Stuttgart, Germany.

[R10] A. Ciechan, K. I. Wysokiński, *„Interorbital pair scattering in clean and impure superconductors"*, presentation at 'The Joint European Magnetic Symposia JEMS 2010', 23-28.08.2010, Cracow, Poland.

Seminars and other presentations (after PhD)

[S1] *„Thermodynamic properties of inhomogeneous multiband superconductors"*, seminar 'Theory and Modeling of Nanostructures' at the Faculty of Physics, University of Warsaw, Warsaw, 31.03.2011.

[S2] *„The influence of pressure on electronic structure of iron superconductors $FeSe_{1-x}Te_x$"*, 'Seminar on Magnetism and Superconductivity' at IP PAS, Warsaw, 18.01.2012.

[S3] *„New generation of conductive phosphoolivine-based cells – band structure calculations"*, presentation at 'II Expert Panel of Project MIME' [G4], Warsaw-Powsin, 19.01.2012.

[S4] *„The effect of pressure and doping on the electronic structure of iron-based superconductors FeSe"*, presentation at th Lublin Scientific Society of the Polish Academy of Sciences, Lublin, 08.11.2012.

[S5] *„Phosphoolivines - Thermal and Magnetic Properties and Band Structure Calculations"*, presentation at 'III Expert Panel of Project MIME' [G4], Warsaw-Powsin, 10.01.2013.

[S6] *„The influence of doping and pressure on the changes in the electronic structure of iron superconductors Fe(Se,Te)"*, presentation at 'KDM Users Reporting Session', Plock, 14-16.05.2013.

[S7] *„Magnetism and Superconductivity of Iron Chalcogenides: Calculations from First Principles"*, presentation at 'Reporting session of the Institute of Physics PAS for 2013', Warsaw, 12.02.2014.

[S8] *„Magnetism and Superconductivity of Iron Chalcogenides: Calculations from First Principles"*, seminar for PhD students at the Institute of Physics UMCS, Lublin, 03.06.2014.

[S9] *„Iron Chalcogenides: Crystallographic, Electronic and Magnetic Structure vs. Superconductivity"*, 'Seminar on Magnetism and Superconductivity' at the Institute of Physics PAS, Warszawa, 04.02.2015.

[S10] *„Magnetic impurities in ZnO: metastability of Mn^{3+} ions and semi-resonant character of Fe ions"*, presentation at Department of Computational Materials Science, Institute of Nuclear Physics PAS, Cracow, 01.03.2016.

[S11] *„Metastability of Mn^{3+} ions in ZnO"*, seminar 'Theory and Modeling of nanostructures', University of Warsaw, Warsaw, 06.10.2016.

[S12] *„Transition metal dopants in ZnO: Mn^{3+} metastability and Fe ion valencey"*, 'Seminar on Magnetism and Superconductivity', Institute of Physics PAS, Warsaw, 14.12.2016.

[S13] *„Transition metal dopants in ZnO"*, 'Seminar on Solid State Physics', University of Warsaw, Warsaw, 31.03.2017.

[S14] *„Transition metal dopants in ZnO"*, presentation at 'XIX ICM Users Reporting Session', Warsaw, 20.04.2017.

[S15] *„Transition Metal Dopants in ZnO: Magnetic and Optical Properties"*, 'Seminar on Magnetism and Superconductivity', Institute of Physics PAS, Warsaw, 05.12.2018.

[S16] *„Transition metal impurities in ZnO: theory of s, p - d exchange coupling"*, 'Seminar on Condensed Matter Physics', Institute of Physics PAS, Warsaw, 28.06.2022.

[S17] *„Transition metal impurities in ZnO: theory of s, p - d coupling"*, 'Seminar on Magnetism and Superconductivity', Institute of Physics PAS, Warsaw, 01.02.2023.

7.5 Review activity

Membership in the journal's editorial committee:

- Acta Physica Polonica A (IP PAS), Associate editor, 2020 - 2024

Reviews of scientific articles in the journals:

- Journal of Physics: Condensed Matter (IOP) - 29 reviews
- Semiconductor Science and Technology (IOP) - 6 reviews
- Journal of Alloys and Compounds (Elsevier) - 10 reviews
- Solid State Communications (Elsevier) - 1 review
- Electronic Structure (IOP) - 2 reviews
- Acta Physica Polonica A (IF PAN) - 18 reviews
- Physica Scripta (IOP) - 7 reviews
- Chemistry Letters (Chemical Society of Japan) - 1 review
- Materials Research Express (IOP) - 2 reviews
- Optical Materials (Elsevier) - 1 review
- Journal of Electronic Materials (Springer) - 1 review
- Modern Physics Letters B (World Scientific) - 2 reviews

Reviewer Awards:

- Journal of Physics: Condensed Matter: 2018 Reviewer Awards (Outstanding reviewer), https://publishingsupport.iopscience.iop.org/questions/journal-of-physics-condensed-matter-2018-reviewer-awards/
- Journal of Physics: Condensed Matter: 2019 Reviewer Awards (Reviewer of the Year), https://ioppublishing.org/news/reviewer-of-the-year-awards-2019/
- Semiconductor Science and Technology: 2020 Reviewer Awards (Outstanding reviewer), https://publishingsupport.iopscience.iop.org/questions/semiconductor-science-and-technology-2020-reviewer-awards/

7.6 Participation in European programmes

- participation in the workshop 'What about U? – Strong correlations from first principles' (17-20.06.2014) as part of the European Union Erasmus+ programme 'Lifelong Learning Programme' (Mobility Type: ERASMUS Staff Mobility - Training for HEI Staff at Enterprises and at HEI), the person receiving: prof. Matteo Cococcioni, Centre Européen de Calcul Atomique et Moléculaire, CECAM-HQ-EPFL, Lausanne, Switzerland.

.....

(applicant's signature)